

FINAL REPORT

Title: Fire Ember Production from Wildland and Structural Fuels

JFSP PROJECT ID: 15-1-04-4

AUGUST 2019

Aixi Zhou, Ph.D., P.E.
North Carolina A&T State University

Stephen L. Quarles, Ph.D.
Insurance Institute for Business & Home Safety

David R. Weise, Ph.D.
Forest Service PSW-Forest Fire Lab-Riverside



FIRESCIENCE.GOV
Research Supporting Sound Decisions



The views and conclusions contained in this document are those of the authors and should not be interpreted as representing the opinions or policies of the U.S. Government. Mention of trade names or commercial products does not constitute their endorsement by the U.S. Government.

Table of Contents

List of Tables 2

List of Figures 3

List of Abbreviations 4

Abstract 6

1. Research Objectives 7

2. Background 7

3. Materials and Methods 8

 3.1 Materials for Thermal Decomposition and Combustion Experiments 8

 3.2 Methods for Thermal Decomposition and Combustion Experiments 9

 3.3. Materials for Firebrand Production Experiments 10

 3.4 Methods for Firebrand Production Experiments 13

 3.5 Firebrand Characterization 17

 3.6. Materials for Experiments on Burning Duration and Intensity of Firebrands 18

 3.7. Methods for Experiments on Burning Duration and Intensity of Firebrands 18

4. Results 20

 4.1. Results for Thermal Decomposition and Combustion Experiments 20

 4.2. Results for Firebrands from Structural Fuels 21

 4.3 Results for Firebrands from Wildland Vegetative Fuels 21

 4.4 Results for Burning Duration and Intensity of Firebrands 22

5. Discussion 28

 5.1 Effect of MC Levels on Pyrolysis and Combustion Properties of Structural Fuels 28

 5.2 Effect of Wind Speed on Firebrand Production and Firebrand Intensity 28

 5.3 Impact of Firebrand Properties on Ignition Potential and Fire Spread in the WUI 29

 5.4 Implications of Results to Standards and Mitigation Related to Firebrand Attacks 30

 5.5 Additional Analysis of Firebrand Data 31

 5.6 Implications for Future Research 31

Literature Cited 33

Appendix A: Contact Information for Key Project Personnel 36

Appendix B: List of Delivery Products 37

Appendix C: Metadata 39

Appendix D: Digital Images for Collected Firebrands 40

Appendix E: Statistical Results for Collected Firebrands 43

List of Tables

Table 1. Selected Structural Fuels and Their Initial Moisture Content (MC) Levels..... 9

Table 2. Structural Assemblies and Testing Wind Speeds* 10

Table 4. Selected Wildland Vegetative Fuels 13

Table 5. Firebrand Parameters for Privacy Fence..... 43

Table 6. Firebrand Parameters for Lattice Fence..... 44

Table 7. Firebrand Parameters for Cedar Siding/Plywood Sheathing Corner Assemblies..... 45

Table 8. Firebrand Parameters for Cedar Siding/OSB Sheathing Corner Assemblies 46

Table 9. Firebrand Parameters for OSB Siding/OSB Sheathing Corner Assemblies..... 47

Table 10. Firebrand Parameters for Recycled Shake Roof Assemblies 48

Table 11. Firebrand Parameters for FRT Cedar Shake Roof/OSB Sheathing Assemblies 49

Table 12. Firebrand Parameters for Non-FRT Cedar Shake Roof/OSB Sheathing Assemblies .. 50

Table 13. Firebrand Parameters for Wall-Roof Mockups: Wood Cladding Only, Combustible Roof..... 51

Table 14. Firebrand Parameters for Wall-Roof Mockups: Wood Cladding Only, Noncombustible Roof..... 52

Table 15. Firebrand Parameters for Wall-Roof Mockups: Wood Cladding Assembly, Combustible Roof..... 53

Table 16. Firebrand Parameters for Wall-Roof Mockups: Wood Cladding Assembly, Noncombustible Roof..... 54

Table 17. Firebrand Parameters for Wall-Roof Mockups: OSB Cladding Only, Combustible Roof..... 55

Table 18. Firebrand Parameters for Wall-Roof Mockups: OSB Cladding Only, Noncombustible Roof..... 56

Table 19. Firebrand Parameters for Wall-Roof Mockups: OSB Cladding Assembly, Combustible Roof..... 57

Table 20. Firebrand Parameters for Wall-Roof Mockups: OSB Cladding Assembly, Noncombustible Roof..... 58

Table 21. Firebrand Parameters for Wall-Roof Mockups: Fiber Cement Cladding Assembly, Combustible Roof..... 59

Table 22. Firebrand Parameters for Wall-Roof Mockups: Fiber Cement Cladding Assembly, Noncombustible Roof..... 60

Table 23. Measured Firebrand Parameters for Little Bluestem Grass..... 61

Table 24. Firebrand Parameters for Chamise 62

Table 25. Firebrand Parameters for Saw palmetto..... 63

Table 26. Firebrand Parameters for Loblolly pine..... 64

Table 27. Firebrand Parameters for Leyland cypress 65

List of Figures

Figure 1. Sketch of A Full-Scale Wall-Roof Mockup Assembly (not to scale) 11

Figure 2. Burning sample (corner assembly) inside the wind tunnel (top left), water pans
downwind of fire (top right), and layout of the water pans (bottom, not to scale). 14

Figure 3. Structural Components Engulfed in Flames During Testing 15

Figure 4. Firebrand Production Experiment - chamise 16

Figure 5. Testing of Cypress Tree at Medium Wind Speed 16

Figure 6. Images Showing Firebrands from Structural (left) and Vegetative (right) Fuels..... 17

Figure 7. Schematic of the Experimental Setup..... 18

Figure 8. Close-up of Smoldering Firebrand Surface Temperature Measurement..... 19

Figure 9. Comparison of Surface Temperatures of Smoldering Firebrands (Wind at 2-m/s) 23

Figure 10. Temperature Variation and the probability of matching the thermocouple
measurements at Different Emissivity Values..... 24

Figure 11. A Sample IR Image from 6-m/s Wind Test..... 24

Figure 12. Average Temperature of the Pixels with $T > 300^{\circ}\text{C}$ 25

Figure 13. Maximum Temperature of Smoldering Firebrands 26

Figure 14. Results of infrared camera of a smoldering firebrand with initial size of 2.5-cm \times 2.5-
cm and wind flow of 3-m/s. 27

Figure 15. Comparison of Mass and Projected Area of Firebrands (95% Confidence Interval).. 30

Figure 16. Representative Digital Images for Firebrands: Corner Assemblies 40

Figure 17. Representative Digital Images for Firebrands: Fences..... 40

Figure 18. Representative Digital Images for Firebrands: Roofs 41

Figure 19. Representative Digital Images for Firebrands: Chamise and saw palmetto..... 41

Figure 20. Representative Digital Images for Firebrands: Southern Yellow Pine and Little
Bluestem Grass 42

Figure 20. Representative Digital Images for Firebrands: Green Cypress and Dry Cypress 42

List of Abbreviations

ASTM	American Society for Testing and Materials
ANOVA	Analysis Of Variance
CDX	Class C to D Exposed (usually used before plywood)
EHC	Effective Heat of Combustion
FR	Flame-Retardant
FRT	Fire-Retardant Treated
HB	Hardboard
HF	Heat Flux
HR	Heating Rate
HRR	Heat Release Rate
IR	Infrared
JFSP	Joint Fire Science Program
MC	Moisture Content
ML	Mass Loss
MLR	Mass Loss Rate
NFPA	National Fire Protection Association
OSB	Oriented Strand Board
PDF	Probability Density Functions
PF	Phenol Formaldehyde
pMDI	Polymeric Methylene Diphenyl Diisocyanate
PU	Polyurethane
RR	Recycled Rubber
SPF	Spruce-Pine-Fir
SYP	Southern Yellow Pine
TGA	Thermogravimetric Analysis
TFO	Time To Flameout
TTI	Time To Ignition
WUI	Wildland-Urban Interface

Keywords

Firebrands, Embers, Wildland Fire, Structures, Structural Fuels, Vegetation, Vegetative Fuels, Firebrand Production, Firebrand Generation

Acknowledgements

This work was supported by the Joint Fire Science Program (JFSP) [Grant ID# 15-1-04-4]. We would like to thank former and current undergraduate and graduate students in the fire research team at the University of North Carolina at Charlotte who assisted with experiments and data collection (in alphabetical order): Fuad Alshammari, Babak Bahrani, Ja’Juan Battle, Noah Bull, Eric Hamman, Faraz Hedayati, Vahid Hemmati, Anurag Jha, Jacob Kadel, William Koch, Gregorio Mesa, and Wenxu Yang. The authors would also like to thank former IBHS colleague Dr. Christine Alfano for assisting the experiments and supplying the samples for this study. We would like to thank the following project collaborator and their contributions: Dr. O.A. “DK” Ezekoye of University of Texas for providing input in research design and planning and for providing Texas prairie grass (little bluestem grass), Dr. Michael J. Gollner of University of Maryland for providing input in research design and planning and for providing assistance in full-scale firebrand production experiments, Casey Grant of the Fire Protection Research Foundation for assistance with input from project technical panel and knowledge transfer to NFPA, Firewise communities, and others.

Abstract

Direct flame contact, radiant heat, and burning firebrands (or embers) have been identified as three principal ways that cause fire spread in the wildland and Wildland-Urban Interface (WUI). However, only burning firebrands can initiate a new spot fire at distances further than 60-m away from the main fire front. During extreme weather events, spotting due to firebrands (referred as the firebrand phenomenon) can overpower fire suppression efforts and become the dominant fire spread mechanism. The spotting process includes three phases: firebrand generation, transportation, and ignition of the recipient fuel. Considerable work on ember transport has been conducted, but much less work has been done to understand fire ember production. Fire ember production from various fuel types under different conditions is the basis for understanding firebrand transport and ignition, and for validating fire behavior models and developing mitigating strategies in the wildland and WUI.

The purpose of this project was to investigate ember production from selected burning wildland and structural (construction materials) fuels under a range of environmental conditions through full-scale and small-scale laboratory experiments. Specific objectives included the determination of thermal decomposition and combustion properties at small scale of selected fuels under a range of heating rate, radiant heat flux, and moisture content (MC) levels, the investigation of firebrand production (including mass, size and flying distance) at full-scale from burning wildland and structural fuels under a range of conditions, the study of burning duration and intensity of embers under a range of conditions, and the evaluation of the impact of key firebrand properties on ignition potential and fire spread in the WUI. Firebrand production is a stochastic phenomenon, thus require a statistical approach to the problem. The outcome variables were ember production properties (such as size, mass and shape, travel distance, burning duration and intensity). The controlling factors were fuel type, fuel MC, fuel geometry and dimension and environmental conditions (e.g., wind speed). Our hypothesis was that the ember production characteristics could be described using thermal and combustion properties and geometry factors of the fuel and would be functions of these controlling factors. We further hypothesized that interaction existed between certain variables involved in the ember production process. Hence correlation among the outcome variables was evaluated. The problem involved observation and analysis of more than one variable at a time, thus linear or non-linear statistical modeling with multiple factors was used.

Results from this project can help us answer the following questions: (1) “What is the rate of ember production from burning wildland and structural fuels in the WUI under a range of wind speed and moisture conditions?”, (2) “What is the characteristic size and shape of embers produced from burning wildland and structural fuels in the WUI under a range of wind and moisture conditions?”, (3) “How far can embers of characteristic size and shape travel under a range of wind speeds?”, (4) “How long can embers of characteristic size and shape burn and at what intensities?”, and (5) “What is the role of ember production from wildland and structural fuels in fire spread in the WUI?”

1. Research Objectives

Spot fires caused by wind-blown burning firebrands (or embers) are a major mechanism of fire spread in the wildland and Wildland-Urban Interface (WUI) [1-6]. Fire spread and structure ignition by embers can be understood in three major processes: ember production, ember transport, and ember ignition of fuel. Considerable work on ember transport has been conducted, but much less work has been done to understand fire ember production and fire ember ignition of fuels. Fire ember production from various fuel types under different conditions is the basis for validating fire behavior models [7-11] and developing mitigating strategies in the wildland and WUI.

Thus, the purpose of the proposed project was to investigate ember production from selected burning wildland and structural (construction materials) fuels under a range of environmental conditions through full-scale and small-scale laboratory experiments. Specific objectives included the following: (1) Determine the thermal decomposition and combustion properties (at small scale) of selected fuels under a range of heating rate, radiant heat flux, and MC levels; (2) Determine the mass and size of embers (at full-scale) from burning wildland and structural fuels under a range of wind speeds; (3) Determine the travel distance of embers as a function of mass, shape and dimensions (at full-scale) under a range of wind speeds; (4) Determine the burning duration and intensity of embers under a range of conditions; and (5) Evaluate the impact of these properties on ignition potential and fire spread in the WUI. The initial research plan included small-scale, intermediate-scale, and full-scale experiments. However, after several trial intermediate-scale and full-scale experiments in 2016, it was determined that the experiments can be performed from small-scale to full-scale directly without going through the intermediate-scale experiments.

2. Background

Burning firebrands (or fire embers) are a critical mechanism of fire spread in large outdoor fires, such as urban fires, wildland fires, and WUI fires. Firebrands are a primary source of ignition in the WUI because they can either directly ignite components of vulnerable structures or can ignite nearby vegetation and other combustibles, which can subsequently ignite the structure via radiant heating or direct flame contact. The firebrand phenomenon (i.e., spotting by airborne burning firebrands) can be understood in three major sequential processes: firebrand generation, firebrand transport, and firebrand ignition of recipient fuel. Firebrands have been studied for some time, most of these studies have focused on spotting distance. To develop scientifically based mitigation strategies for WUI fires, it is necessary to understand the firebrand generation process.

Firebrand generation is the first step of the firebrand phenomena and is the basis for understanding the subsequent transport and ignition processes. A limited number of experimental studies have been performed on firebrand production over the past several decades [12-34]. The number of samples collected in most previous firebrand generation experiments varied between 50 and 500 firebrands. This has been a source of uncertainty and brings limitations on how much information the collected firebrands can provide about the whole population. The vital question is how many firebrands are needed to sufficiently quantify the characteristics of the entire population of the firebrands in an experiment. If the answer suggests a sample size far larger than 500, the efficiency of the current measurement methodology to count and measure thousands of firebrands must be explored. To address this issue, this study developed a new statistics-based framework that incorporates a machine learning predictive model for the sampling and measurement processes in

firebrand generation experiments so that the obtained firebrand data can achieve the desired level of statistical reliability with increased efficiency [35].

Firebrand production is affected by many factors, such as the fuel material type, condition of the fuel (e.g., live or dead fuels and moisture content levels), the thermal degradation characteristics (or pyrolysis properties) of the fuel, the combustion properties of the fuel, and environmental conditions the fuel is subjected to (such as wind, relative humidity, temperature, and external heating condition). These factors will affect the outcome variables in the firebrand production process, such as the possibility of firebrand formation, firebrand production rate, the physical characteristics of firebrands (e.g., firebrand size, mass, and travel distance) and the combustion characteristics of firebrands (e.g., burning duration and intensity, potential heat energy, temperature and heat flux). Particularly, there is a need for specific information relating basic structural (dimensions), pyrolysis and combustion properties of the fuel with the firebrand production process and the associated physical and combustion characteristics of the produced firebrands. These existing ember production studies have been conducted on a limited number of wildland and structural fuels under limited fuel moisture content (MC) levels and environmental conditions [36]. Effect of conditions such as seasonal differences on the combustion characteristics of vegetative fuels has been reported [37-38]. However, only a limited number of publications has addressed structural fuels. One of the objectives of this project was to determine the pyrolysis and combustion properties of selected structural fuels (construction materials) in typical residential buildings in the U.S.

3. Materials and Methods

3.1 Materials for Thermal Decomposition and Combustion Experiments

Wood and wood-based composites are widely used in residential construction in the US. Structural fuels were selected using the criteria that the chosen materials should be representative of typical residential building construction materials in wildfire prone areas in the U.S. In addition, the selected fuels should cover a range of building components, including framing, sheathing, siding, and roofing. This led to the following seven structural fuels for this study: southern yellow pine (SYP) and spruce-pine-fir (SPF) as representative framing lumber materials, two types of oriented strand board (OSB) materials and one CDX grade of plywood as representative sheathing materials, and a hardboard (HB) and an OSB as representative combustible siding materials. The identification, description and short name of each selected material are shown in Table 1. Materials A and B are natural woods, and Materials C-G are engineered wood composites. These materials were purchased either from a home improvement store (Lowe's), or directly from the product manufacture. The products were then processed to appropriate dimensions as specimens for the study.

The initial MC levels in the as-received structural fuels were determined using the procedures described in the primary oven-drying method outlined in ASTM D4442 [39]. The obtained initial MC levels for the selected materials are shown in Table 1. The initial MC levels of the selected materials were in the 11-15% range for natural woods (Materials A and B) and the 3.5-8.0% range for wood-based composites (Materials C-G). For the purpose of this study, three nominal MC levels were selected to examine the effect of MC level on thermal degradation and combustion properties: 5%, 10%, and 15%. More details about the procedures to achieve the nominal MC levels can be found in [36]. When a sample achieved a pre-determined nominal MC level, it was

sealed by two layers of heavy-duty plastic bags for storage and the mass of the sample was measured and recorded periodically to monitor any change in mass before testing. Results showed that the storage method was effective in maintaining the target MC in the conditioned specimens prior to testing.

Table 1. Selected Structural Fuels and Their Initial Moisture Content (MC) Levels

ID	Material Description and Short Name	MC (%)
A	Southern Yellow Pine frame lumber (SYP)	13.5
B	Spruce-Pine-Fir framing lumber (SPF)	11.7
C	OSB Sheathing with PF ¹ face and pMDI ² core (OSB-PF)	7.8
D	OSB Siding with pMDI adhesive (OSB-Siding)	3.5
E	OSB Sheathing with pMDI adhesive (OSB-pMDI)	6.0
F	Sheathing Plywood (CDX grade) with PF adhesive (CDX)	7.3
G	Hardboard Siding (HB)	5.7

1. Phenol Formaldehyde adhesive. 2- polymeric Methylene Diphenyl Diisocyanate adhesive.

3.2 Methods for Thermal Decomposition and Combustion Experiments

The dimensions (length, width, and thickness) and mass of selected specimens were measured to determine the change in volume and density of the material as a function of MC. The density at a MC level was based on the mass of a specimen, including moisture and its volume at the MC level, as per ASTM D2395 [40], i.e., the density of a material was determined on a current mass / current volume basis by dividing the mass (in grams) to the volume (in cm³) of the specimen at a specific MC level.

The thermal conductivity of the selected fuels was measured by using the TA Instruments Fox 50 heat flow meter. Experiments were performed per ASTM C518 procedures [41] at two temperature levels (25 °C and 100 °C) at each MC level. The specimens for Fox 50 were required to be cylinder (thickness < 25.4mm, and 50mm < diameter < 62mm). Thus the TGA samples were cut down into 20mm thickness and 55mm diameter cylinders, and conditioned to the 5%, 10%, 15% nominal MC level prior to testing. Three replicated tests were performed at each temperature and MC level combination.

The pyrolysis properties of the selected fuels were measured through Thermogravimetric Analysis (TGA) by using the TA Instruments Q600 SDT analyzer. TGA can be performed through an isothermal process or a non-isothermal process. The isothermal process uses constant temperatures while the non-isothermal process ramps the temperature from ambient to the target temperature at a given heating rate (HR). In order to determine the pyrolysis kinetics over a range of heating conditions, the TGA experiments were performed using the non-isothermal method at three HR levels (5, 15, and 25 K/min) at each MC level. The thermal degradation kinetics were primarily measured by mass loss and mass loss rate. Granule samples were cut down from the properly conditioned cylinder-shaped specimens for the thermal conductivity measurement, and then were tested in a nitrogen atmosphere with a purge rate of 20 mL/minute. Three replicated tests were performed for each HR and MC level combination.

Fire Ember Production from Wildland and Structural Fuels

The combustion properties of the selected fuels were measured by using a cone calorimeter. In order to determine the combustion properties over different external heating conditions, the cone calorimeter experiments were performed at three heat flux (HF) levels: 20, 30 and 50 kW/m² at each MC level. Three replicates at each HF level and MC level combination were tested. ASTM E1354 [42] was used for specimen preparation, testing, and protocol for data collection [36,43].

3.3. Materials for Firebrand Production Experiments

3.3.1 Structural Fuels

The selection of structural assemblies for full-scale firebrand production experiments was based on the following criteria: (1) They should be representative of typical residential building construction in wildfire prone areas in the US and have high possibility of producing firebrands; (2) They should cover a range of residential building structural assemblies; (3) The number of structural components or assemblies should be manageable for the team to test in the wind tunnel facility. The following table lists the selected structural assemblies, their labeling ID in our tests and data analysis, testing wind speed, and the number of firebrands measured.

Table 2. Structural Assemblies and Testing Wind Speeds*

Component	Sheet Label	Material	Wind Speed
Fence (F)	F-P-I	Privacy (P)	Idle (I)
	F-P-M		Medium (M)
	F-P-H		High (H)
	F-L-I	Lattice (L)	Idle
	F-L-M		Medium
	F-L-H		High
Corner (C)	C-CP-I	Cedar/Plywood (CP)	Idle
	C-CP-M		Medium
	C-CP-H		High
	C-CO-I	Cedar/ OSB (CO)	Idle
	C-CO-M		Medium
	C-CO-H		High
	C-OO-I	OSB Siding/ OSB Corner (OO)	Idle
	C-OO-M		Medium
	C-OO-H		High
Roof (R)	R-RR-I	Recycled Rubber (RR)	Idle
	R-RR-M		Medium
	R-RS-H		High
	R-NFS-I	Non-FRT Shake (NFS)	Idle
	R-NFS-M		Medium
	R-NFS-H		High
	R-FS-I	FRT Shake (FS)	Idle
	R-FS-M		Medium
R-FS-H	High		

*: Corner (C) refers to a wall/siding assembly.

Fire Ember Production from Wildland and Structural Fuels

Fence samples included privacy and lattice types. In a privacy fence, vertical fencing planks (nominal one-inch thick board) were placed side-by-side and attached to the same side of the horizontally oriented structural support system. In a lattice fence, diagonal slats were arranged in crisscross patterns. Roofs were 24" wide, 2X4 framing, 24" on center. In roof assemblies, roof coverings were Fire-Retardant Treated (FRT) and non-FRT wood shakes and a recycled rubber covering. Roof sheathing is ½" CDX grade plywood. The corner assemblies were built from typical residential building construction materials in wildfire prone areas of the United States. A re-entrant corner assembly was used to evaluate siding assemblies as this was felt to result in most severe exposure as it restricts the air flow and limits the transport distance. Corners were made with solid or composite wood horizontal lap attached to a ½-in. OSB or CDX plywood sheathing. Each wall in the corner assembly was 32-in. (81-cm) long, using 2-in.×4-in. (5-cm×10-cm) southern yellow pine (SYP) framing, 16-in. (41-cm) on center. A nominal ½-in. (1.3-cm) gypsum board was attached to the non-fire exposed walls. Wall sheathing on the fire-exposed side was nominal ½-in. (1.3-cm) OSB. Siding on the fire exposed side was solid cedar wood. All the samples were conditioned in a kiln to reach the nominal moisture content of 5% prior to the firebrand production experiments.

A sketch of a full-scale wall-roof mockup assembly is shown in Figure 1. The full-scale mockup structural assembly includes a wall, its cladding, and a roof. The back of the assembly is open (no insulation). Samples were conditioned in a kiln to reach the nominal moisture content of 5% prior to experiments. Note that this is the diagram for Phase II siding tests, not the roof test. The red vertical and horizontal lines represent location of gas burners. The comment "Need to price cost of siding ..." should be deleted as it is a note to the research group. A summary of the tested structural assemblies is shown in Table 3.

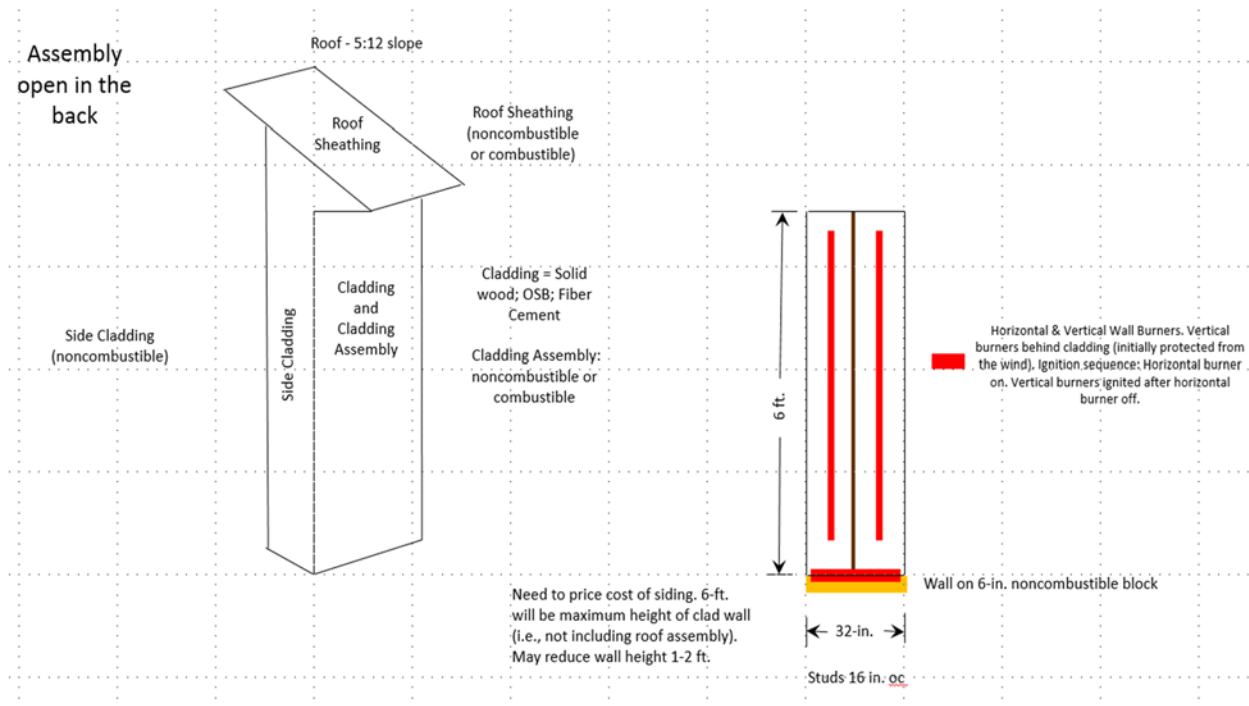


Figure 1. Sketch of A Full-Scale Wall-Roof Mockup Assembly (not to scale)

Fire Ember Production from Wildland and Structural Fuels

Table 3. Summary of Wall-Roof Assemblies and Testing Wind Speeds

Cladding	Wall Type	Material	Roof (Sheathing)	Wind Speed (I, M, H)	Sheet Label
Solid Wood (Cedar)	Cladding Only	Wood Stud; No sheathing; Cedar siding attached directly to stud	Combustible Sheathing	I	S-CL-NC-CS-I
			Non-Combustible Gypsum Panel		S-CL-NC-NCS-I
	Assembly	Wood Stud; 7/16" OSB Wall Sheathing; Cedar Siding	Combustible Sheathing		S-A-C-CS-I
			Non-Combustible Gypsum Panel		S-A-C-NCS-I
	Cladding Only	Wood Stud; No sheathing; Cedar siding attached directly to stud	Combustible Sheathing	M	S-CL-NC-CS-M
			Non-Combustible Gypsum Panel		S-CL-NC-NCS-M
	Assembly	Wood Stud; 7/16" OSB Wall Sheathing; Cedar Siding	Combustible Sheathing		S-A-C-CS-M
			Non-Combustible Gypsum Panel		S-A-C-NCS-M
	Cladding Only	Wood Stud; No sheathing; Cedar siding attached directly to stud	Combustible Sheathing	H	S-CL-NC-CS-H
			Non-Combustible Gypsum Panel		S-CL-NC-NCS-H
	Assembly	Wood Stud; 7/16" OSB Wall Sheathing; Cedar Siding	Combustible Sheathing		S-A-C-CS-H
			Non-Combustible Gypsum Panel		S-A-C-NCS-H
OSB	Cladding Only	No sheathing; OSB siding	Combustible Sheathing	I	OSB-CL-OSB-CS-I
			Non-Combustible Gypsum Panel		OSB-CL-OSB-NCS-I
	Assembly	7/16" OSB wall sheathing; Cedar siding	Combustible Sheathing		OSB-CL-OSB.CED-I
			Non-Combustible Gypsum Panel		OSB-CL-OSB.CED-I
	Cladding Only	No sheathing; OSB siding	Combustible Sheathing	M	OSB-CL-OSB-CS-M
			Non-Combustible Gypsum Panel		OSB-CL-OSB-NCS-M
	Assembly	7/16" OSB wall sheathing; Cedar siding	Combustible Sheathing		OSB-CL-OSB.CED-M
			Non-Combustible Gypsum Panel		OSB-CL-OSB.CED-M
	Cladding Only	No sheathing; OSB siding	Combustible Sheathing	H	OSB-CL-OSB-CS-H
			Non-Combustible Gypsum Panel		OSB-CL-OSB-NCS-H
	Assembly	7/16" OSB wall sheathing; Cedar siding	Combustible Sheathing		OSB-CL-OSB.CED-H
			Non-Combustible Gypsum Panel		OSB-CL-OSB.CED-H
Fiber-Cement	Assembly	7/16" OSB wall sheathing; Fiber cement siding	Combustible Sheathing	I	FC-A-OSB.FC-CS-I
			Non-Combustible Gypsum Panel		FC-A-OSB.FC-NCS-I
			Combustible Sheathing	M	FC-A-OSB.FC-CS-M
			Non-Combustible Gypsum Panel		FC-A-OSB.FC-NCS-M
			Combustible Sheathing	H	FC-A-OSB.FC-CS-H
			Non-Combustible Gypsum Panel		FC-A-OSB.FC-NCS-H

3.3.2. Wildland Vegetative Fuels

Criteria for the selection of wildland vegetative fuels were: (1) they should be representative of typical wildland vegetative fuels in the U.S. that are prone to ignition and firebrand generation; (2) they should be accessible to experimental teams in NC and SC at reasonable costs (or to research partners in Texas and California). The following wildland vegetative fuels were used in this study: Chamise (*Adenostoma fasciculatum*) and saw palmetto (*Serenoa repens*) as shrubs, loblolly pine (*Pinus taeda*) and Leyland cypress (*Cupressus x leylandii*) as trees, and little bluestem grass (*Schizachyrium scoparium*) for grass samples. Live saw palmetto samples were collected from the Victoria Bluff Heritage Preserve/Wildlife Management Area in Bluffton, SC. Loblolly pine trees were harvested on IBHS property in Richburg, SC. Leyland cypress samples were harvested from a tree farm in Chester County SC for Phase I vegetation tests in 2016, and on IBHS property for Phase II vegetation tests in 2017. Chamise samples were collected from the North Mountain Experimental Area near Riverside, CA, and shipped to the IBHS Research Center in Richburg, SC. Little bluestem grass samples were collected from Texas and shipped to the IBHS Research Center. Table 4 provides basic information about the selected wildland vegetative fuels.

Table 3. Selected Wildland Vegetative Fuels

Vegetation Level	Vegetation Type	Collection Site	Average Moisture Content (%)			Test Day
			Needle	Twig	Branch	
Grass	Little bluestem grass	Texas	<i>Not Recorded</i>			
Shrubs	Chamise*	Southern California	<i>Not Recorded</i>			20.3
	Saw palmetto	Coastal Area of South Carolina	<i>Not Recorded</i>			59.9
Trees	Loblolly pine	South Carolina	107.6	130.8	175.4	8.8
	Leyland cypress		106.9	100.7	95.1	10.4

* Cut into branches and reassembled into cylindrical wired form prior to testing.

3.4 Methods for Firebrand Production Experiments

Tests were performed in the test chamber at the Insurance Institute for Business & Home Safety (IBHS) Research Center in Richburg, South Carolina. The facility has a 148-ft. × 148-ft (45-m × 45-m) open-jet wind tunnel with a clear height of 59-ft. (18-m). The wind flow is produced using arrays of 105 approximately 6-ft. (1.8-m) diameter fans with active and passive control elements

Fire Ember Production from Wildland and Structural Fuels

to simulate atmospheric boundary layer flow up to 130-mph (58-m/s) wind speeds 33-ft. (10-m) above the ground. Two of the three designated wind speed levels used in the experiments were fluctuating (Medium and High) and one (Low) was constant: Low (average 12-mph or 5-m/s), Medium (average 25-mph or 11-m/s), and High (average 40-mph or 18-m/s). The 3-s gust peaks were 14.3-m/s, and 23-m/s for the medium and high wind traces, respectively.

Fuel packages were ignited with custom-build natural gas burners. Slotted natural gas burners were positioned to enable ignition of the assemblies at the base (bottom). Flames impinged at the bottom of siding and leading edge of roof assemblies. Fence samples were held in a vertical orientation, and corner assemblies were oriented such that the corner was open at 45° to the wind direction. Testing times were 15-min and 35-min for privacy fence and lattice fence, respectively. Also, average testing time for corner and roof assemblies were 15-min and 30-min, respectively.

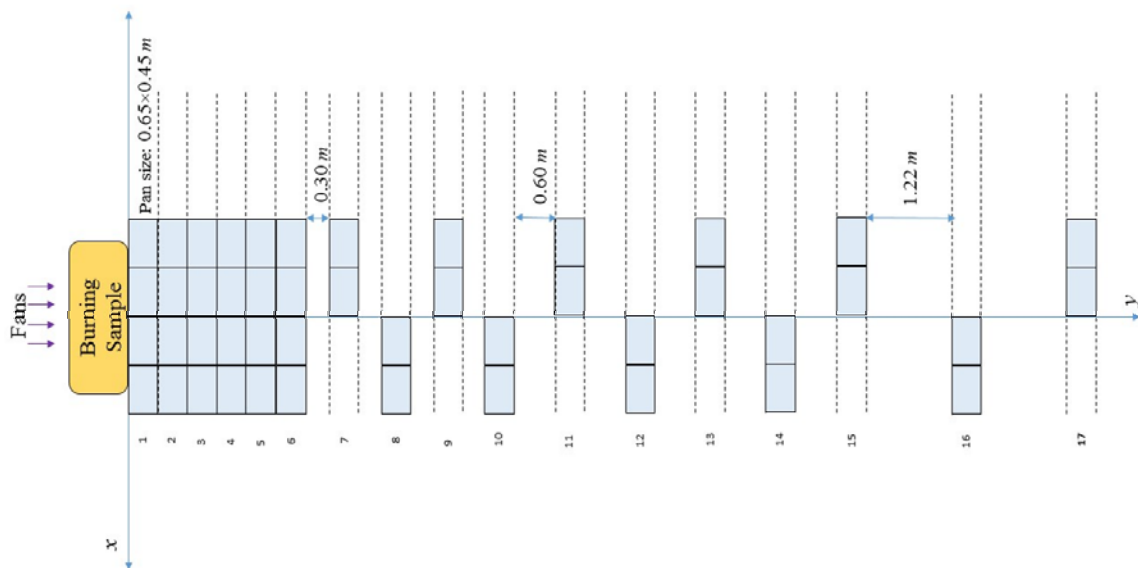


Figure 2. Burning sample (corner assembly) inside the wind tunnel (top left), water pans downwind of fire (top right), and layout of the water pans (bottom, not to scale).

Fire Ember Production from Wildland and Structural Fuels

All samples were weighed immediately before and after the test. Tests were conducted using three different wind traces. Two replicates for each assembly were used in each wind speed. Firebrands were collected in water-filled pans. Figure 2 shows a burning sample (corner assembly) inside the wind tunnel, the layout of the water pans, and water pans downwind of fire during testing.

A rectangular area of approximately 2-m \times 15-m downwind of fire specimen was available in the test chamber for water pans. Wake flows immediately downwind of the object are strong which may cause many firebrands to land a short distance from the burning object so six rows of pans were placed immediately downwind of the fuel package. Assuming a symmetrical distribution of firebrands about the central line water pans were located on alternate sides for rows 6 through 17 to maximize distance covered. In total, 46 aluminum water pans, each with a capture area of 0.65-m \times 0.45-m, were strategically located to optimize collection of firebrands. Window screens (mesh) were submerged in each water pan to facilitate the collection of firebrands.

Figures 3a-3d show different structural assemblies engulfed in flames during testing. Figure 4 shows two pictures during firebrand production experiment for Chamise. Two ignition sources were used for vegetative fuels: 1) natural gas burned for 10-s for trees and blue stem grass, and 2) pine needle bed for Palmetto and Chamise samples. Figure 5 shows snapshots of testing of Cypress tree at medium wind speed.



(a) Privacy Fence



(b) Cedar Siding/OSB Sheathing Corner Assembly



(c) Non-FRT Cedar Shake Roof / OSB Sheathing



(d) FRT Cedar Shake Roof / OSB Sheathing

Figure 3. Structural Components Engulfed in Flames During Testing

Fire Ember Production from Wildland and Structural Fuels



Figure 4. Firebrand Production Experiment - chamise



(1) Leyland cypress-front view



(2) Leyland cypress-side view



(3) Flame Impingement



(4) Ignition/ Firebrand Generation



(5) Tree Stem after the Test



(6) Collection Pans

Figure 5. Testing of Cypress Tree at Medium Wind Speed

Collected firebrands were then transferred to an oven maintained at 103°C for at least 24-hours to remove moisture from the sample. The oven-dried firebrands were stored in sealed plastic bags and clearly marked for each test. The number of firebrands in one bag was intentionally limited to ensure that only one layer of firebrands was stored in one bag. The bags were separated from each other with layers of paper towels and were gently placed in boxes to avoid firebrand breakage during transportation to the University of North Carolina at Charlotte. Although extreme care was taken during transportation and handling, some of them might have been broken. We recognize this is a source of uncertainty in this study.

3.5 Firebrand Characterization

Three key parameters of firebrand are traveling distance, mass, and projected area. Traveling distance represents the horizontal distance from the point the firebrand was generated to where it lands. For these tests the travel distance can be calculated by over the straight length of the straight line from the burning corner assembly to the center of the collection pan which is known by the row and column (as shown in Figure 6.b). The mass of the firebrand changes from when it is generated from the source fuel as it burns, and virgin fuel combusts. When the firebrand lands the water quenches the combustion and stops mass loss. Individual firebrands were weighted using a digital balance (Sartorius H51, resolution of ± 0.0001 gram).

The size and shape of firebrands can impact the aerodynamics during transport and accumulation geometry. In the literature, there is not much detail about the calculation of the surface area of the firebrands. A new process was developed to expedite measuring the projected area of firebrands. Firebrands were placed on a white sheet of paper which provided a contrasting background to black (firebrand) objects. High-resolution pictures were captures of each sheet using a Nikon D5600 and light setup that provided adequate lighting from three directions at 120 degrees interval on the sheet to avoid shadows. Figure 6 shows typical digital images of firebrands. More digital images are provided in Appendix D. To increase the efficiency in measuring the projected area and minimize human labor, a MATLAB code was developed to automate the process as described in detail in [35]. Using this automated method, counting and calculating the projected area of hundreds of firebrands can be accomplished in a few seconds.



Figure 6. Images Showing Firebrands from Structural (left) and Vegetative (right) Fuels

3.6. Materials for Experiments on Burning Duration and Intensity of Firebrands

To investigate the burning duration and intensity of firebrands, square OSB samples were prepared and placed in a small-scale firebrand generator [44]. Surface temperature of smoldering firebrands was used as a key physical parameter to quantify burning duration and intensity of firebrands. Smoldering firebrands were generated by exposing the OSB samples to a propane flame until fully involved and allowing the flaming combustion to cease (flameout) before the sample was ready for testing. Experimental results from [45] showed the average projected area of firebrands from structural fuels was 4.87 cm^2 ; hence, firebrands were generated in a way that their initial projected area represented a similar area. Each side of the firebrand was approximately 23-mm after flameout ($\sim 5\text{-cm}^2$ projected area).

3.7. Methods for Experiments on Burning Duration and Intensity of Firebrands

Accurate measurement of the surface temperature of a smoldering firebrand has been challenging. Different techniques such as contact methods using thermocouples and non-contact methods using optical devices such as infrared (IR) devices have been employed for this task. In theory, optical devices are accurate and are more convenient due to their ability to analyze a larger area compared to thermocouples, which only measure temperature at the contact points. In practice, however, the IR devices require the user to accurately set a surface emissivity. As part of this study, the proper range of emissivity for IR imaging cameras was determined and used to measure the surface temperature of smoldering firebrands. One spot on the firebrand was monitored using thermocouples, an IR pyrometer, and an IR camera, as shown in Figure 7.

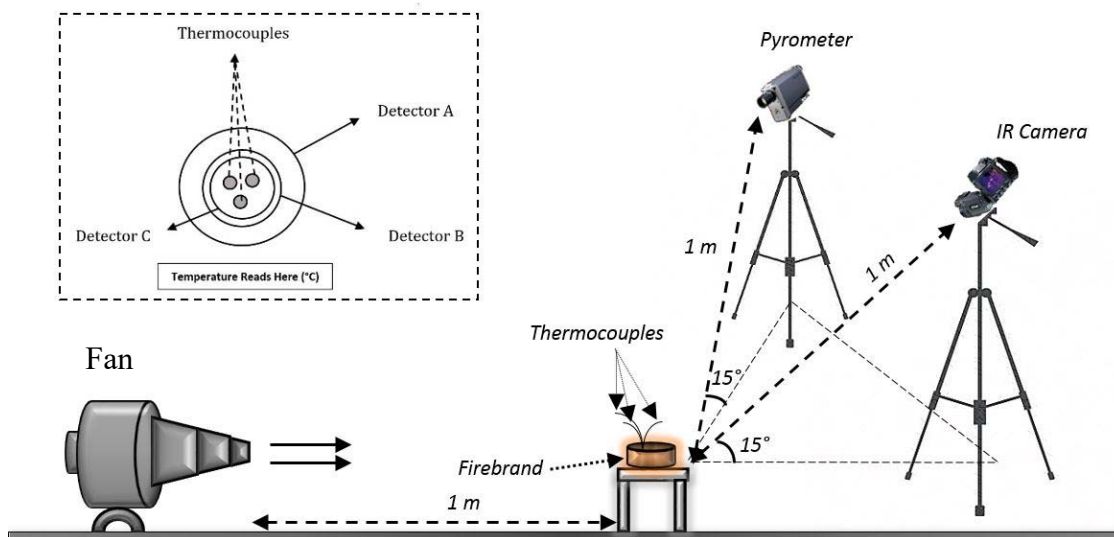


Figure 7. Schematic of the Experimental Setup

The emissivity was adjusted to minimize the difference between the average thermocouple readings and that of the IR camera. Changing the emissivity value for the IR camera measurements, different temperature curves were obtained, and a Gaussian probability density function was constructed to find the likelihood of matching the infrared temperature readings at each emissivity with that of from thermocouples. After the proper emissivity range was determined, we then measured the surface temperature of smoldering firebrands using a thermal IR camera, and analyze

the surface temperature profiles of smoldering firebrands using the obtained data. Figure 8 shows a close-up view of the surface temperature measuring process.

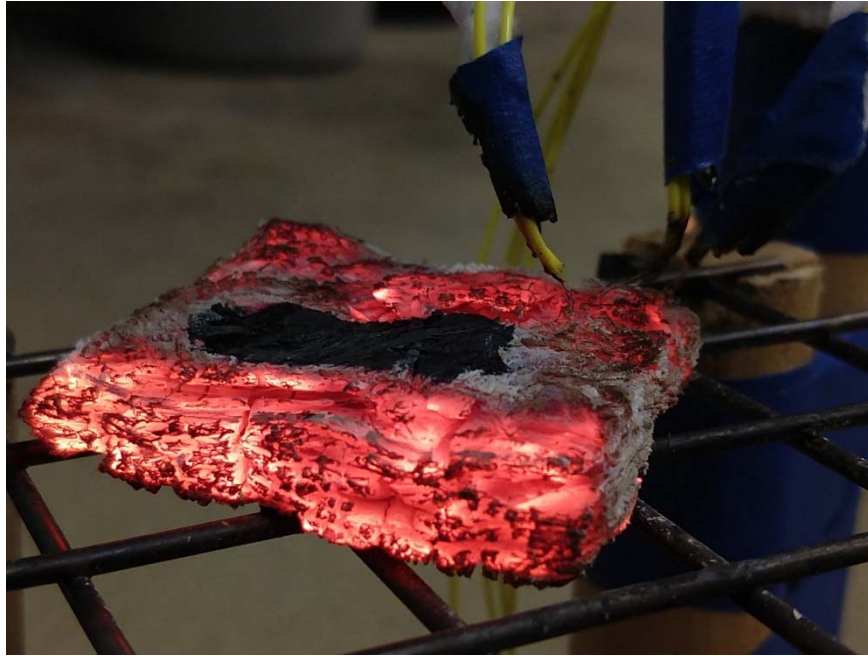


Figure 8. Close-up of Smoldering Firebrand Surface Temperature Measurement

As shown in Figure 7, three OMEGA[®] Precision Fine Wire type K thermocouples with 0.125-mm bead diameter (response time 1.0 second) were utilized for measurements. Simultaneously, a *long range* Heitronics[®] KT 19.81 II pyrometer (operation range 8-12 μm) and a *long range* FLIR[®] T620 IR camera (operation range 7.5-14 μm) were aimed on the same spot as where the thermocouples were located (see Figure 1). The IR camera has two temperature calibration ranges: 100-650°C and 300-2000°C. The temperatures below 300°C were sacrificed in favor of the ones above 300°C since typically a higher temperature translates to firebrands with greater ignition potential. This decision had to be made due to hardware limitations. The smoldering firebrands were then placed on a wire grid which was placed almost perpendicularly 1-m beneath the camera.

The continuous change of temperature and condition on the surface of a smoldering firebrand makes it difficult for surface temperature measurement using thermocouples. In addition to the high surface temperature, a smoldering firebrand shrinks non-uniformly over time which makes the receding of the surface in a random fashion. Moreover, the smoldering firebrand could become fissured, which may lead to loss of proper contact between the thermocouple tip and the surface. In order to overcome this issue, a retaining mechanism was designed to continuously apply force to the thermocouple tips in the direction of the specimen's surface. As the firebrand size decrease, the mechanism exerted force on thermocouples to push it towards the firebrand surface to compensate the burned volume. It was observed during experiments that any change on the specimen's surface (e.g. cracking) that resulted in dislocation of the thermocouples' tips (even slightly), the standard deviation of surface temperature was dramatically increased (>150°C). Using this setup, the junctions were continuously in a proper contact with the firebrand's surface, shown in Figure 8.

A total of 40 experiments were conducted to ensure the repeatability of the experimental procedure. The blower was turned on during the experiment at 20-s to 40-s and 90-s to 100-s, generating a 2-m/s and 6-m/s wind to the surface, respectively. The wind caused fluctuations in surface temperature which was not traceable by the thermocouples due to their slower response time. However, the pyrometer was able to record the variations of surface temperatures. One limitation of utilizing thermocouples for surface temperature measurement was their thermal equilibrium loss with the surface in presence of wind. Acceptable agreement between the thermocouples and pyrometer readings, $\pm 25^{\circ}\text{C}$, in absence of wind showed the emissivity is close to unity. Temperature data from the FLIR IR camera were processed using the camera's software, Research IR®, to examine the effects of changes in emissivity values on temperature.

4. Results

4.1. Results for Thermal Decomposition and Combustion Experiments

The Flynn-Wall and Ozawa method (or the FWO method) per ASTM E1641 was used for analyzing non-isothermal thermal decomposition TGA data in this study. The data collection and analysis procedures in ASTM E1354 were used for collecting and analyzing combustion properties. All data points were the average from at least three replicates. Both average and standard deviation values are reported for all data. The obtained density, thermal conductivity and combustion property data were analyzed via a simple ANOVA process in MATLAB (version R2017b) using a 95% confidence interval. In the ANOVA analysis of thermal conductivity and combustion property data, the MC levels changed from 5% to 10% and 15% while other parameters such as temperature and heat flux levels were kept constant. Values show statistically significant difference between the means are noted or highlighted in the tables. Although the cone calorimeter tests measured many combustion properties, only the following relevant combustion properties will be reported in this study: time to ignition (TTI), heat release rate (HRR, including the peak heat release rate (PHRR) and the average heat release rate (AHRR) over 180 seconds after ignition), mass loss (ML) and mass loss rate (MLR), effective heat of combustion (EHC), and time to flameout (TFO). Article [36] reported the following results from the thermal decomposition and combustion experiments: material density and thermal conductivity, pyrolysis properties, and combustion properties. The reported study investigated the effects of MC levels (5%, 10%, and 15%) on the pyrolysis and combustion properties of selected structural fuels under a range of external heating rates and radiant heat flux levels.

This study demonstrated that MC levels changed the density of the materials. Based on a 95% confidence interval, the density for natural woods changed more significantly compared to that of engineered woods. All materials except E and F had statistically significant increase in density when the MC levels increased from 5% to 15%. When density is calculated in a current mass / current volume basis, one would expect density to increase with moisture content. The difference between wood and engineered wood products could be explained by cross lamination that occurs in plywood and OSB products which would restrict volume change as a function of change in moisture.

The thermal conductivity values for most of the materials increased as MC level increased, but the increase was not always statistically significant. All materials, except B at 25 °C and E at 100 °C, had no statistically significant change in thermal conductivity when the MC levels increased from 5% to 10% at 25 °C and 100 °C.

The pyrolysis properties were affected by both the MC levels and heating rate levels. The pre-exponential factor and activation energy values varied in the early stage of the pyrolysis, but appeared to be more stable when the conversion factor α became 0.25 or higher. Both MC level and heating rate had strong effect on the pre-exponential factor for all materials.

Within the studied ranges, both the MC levels (5-15%) and the HF levels (20-50 kW/m²) affected the combustion properties. Statistical analysis of combustion data using a 95% confidence interval showed that when the HF was kept constant and the MC increased from 5% to 15%, TTI increased significantly at low HF (20 kW/m²), but the increase became small at medium HF (30 kW/m²) and negligible at high HF (50 kW/m²).

4.2. Results for Firebrands from Structural Fuels

Physical quantities of generated firebrands from fence, interior corner siding, and roof assemblies are summarized in Tables 5 to 12 in Appendix E. Physical quantities of generated firebrands from full-scale wall-roof mockup assemblies are summarized in Tables 13 to 22 in Appendix E.

In addition to mean, standard deviation, median, and correlation values, the skewness of each parameter is also provided. Skewness is an important parameter in studying probability distribution function asymmetry. A positive skew indicates the mass of the distribution is concentrated on the left of the figure, i.e., the distribution is right-skewed or right-tailed. All skewness values for flying distance, projected area and mass are positive. Thus, the distributions of these parameters are right-skewed. Correlation value of positive one indicates a direct relationship between the parameters while negative one indicates an inverse relationship. Zero correlation means no relation between the parameters exists. The correlation values in the tables show that mass and projected area are strongly correlated, as observed in some experimental and theoretical studies [35] The corrections between mass and traveling distance as well as projected area and traveling distance are small. The mean and median of travel distance, projected area, and mass increased as wind speed increased. Wind speed can have competing effects on generation of firebrands, in that higher wind speeds can force departing larger firebrands (increasing production rate and size) and at the same time will increase the combustion rate during the flight (reducing size). Since the flying distance in this experiment was limited by the dimensions of the test chamber, results suggested that stronger wind caused larger firebrands to depart which traveled further away. Also, the standard deviation of projected area and mass increased when wind speed increased, which implies that the range of variation in the size and mass of the firebrands was larger under stronger winds (more variability in the sample).

Among different structural assembly types, roof tended to generate larger and heavier firebrands compared to fences, and corner assemblies. For the two different types of fence, firebrands from lattice fence are smaller and lighter than those from private fence. However, additional data analysis should be performed to provide more insight on these comparisons.

4.3 Results for Firebrands from Wildland Vegetative Fuels

The data reported includes physical property information of generated firebrands, including mass, projected area, and flying distance from selected vegetative fuels in whole-plant laboratory experiments. Physical quantities of generated firebrands from grass, shrubs, and trees are summarized in Tables 23 to 27 in Appendix E.

Among all these wildland vegetative fuels, firebrands from little bluestem grass were the smallest and lightest. Chamise firebrands were the largest and heaviest. Saw palmetto firebrands were large in projected area, but light in weight. Compared to structural firebrands, vegetative firebrands were generally smaller and lighter. Further data analysis can provide a better understanding of this kind of comparison.

Firebrands from vegetative fuels show strong correlation between mass and projected area, while the correlation between flying distance and area as well as mass are small. The skewness values for the three parameters (flying distance, projected area and mass) are all positive, indicating the right-skewed distributions of these parameters. In general, the mean and median of flying distance, projected area, and mass increased as wind speed increased. Therefore, higher wind speed generated larger and heavier firebrands. The standard deviation of projected area and mass increased as wind speed increased, implying larger variation ranges in the size and mass under stronger winds.

4.4 Results for Burning Duration and Intensity of Firebrands

Figure 9 shows the recorded values of the thermocouples and the pyrometer and their difference in readings. The emissivity of the pyrometer for these tests was set to 1.00. The circles show the average values of the three thermocouples and the black bars are their standard deviation values. As can be seen in Figure 10, increasing the emissivity from 0.60, temperatures measured using the IR camera decreased. The temperatures differences between the thermocouples and the IR camera became smaller and smaller as the emissivity increased to 1.00.

Considering the emissivity as a discrete random variable, the expected value for emissivity can be calculated by employing probability density functions (PDFs). Assuming the probable error of the mean is normally distributed, a normal distribution PDF was constructed with thermocouples' measurements in 5-s time intervals. It should be mentioned that one can try other PDF types other than normal distribution.

$$\varepsilon = \frac{\sum \varepsilon(i)PDF(i)}{\sum PDF(i)} \quad \text{Eq. (1)}$$

Equation (1) describes the expected value for emissivity, where $\varepsilon(i)$ is the emissivity and $PDF(i)$ is its associated probability. The normal PDFs were constructed with the mean and standard deviation of the thermocouples' measurements at each time. Finally, averaging emissivity in each experiment, the mean value of emissivity was determined to be 0.97, with a standard deviation of 0.05. Furthermore, using a 99% confidence interval, the emissivity values for the smoldering firebrands were determined to be between 0.91 and 1.00.

The temperature variation for several smoldering firebrands were analyzed. Increasing the emissivity from 0.10 to 1.00, the local temperature (the spot monitored by thermocouples) at each time interval was extracted and plotted in Figure 10 for each IR image. This figure also graphically depicts the employed technique to find the emissivity range. The most probable value for emissivity can be achieved by matching the epsilon to the thermocouple measurements. The lowest the epsilon gets, the lower probability of matching the infrared measurement with the thermocouples. As can be seen, emissivity value of less than 0.85 can bring large discrepancies in temperature measurements from the thermocouples and the IR camera.

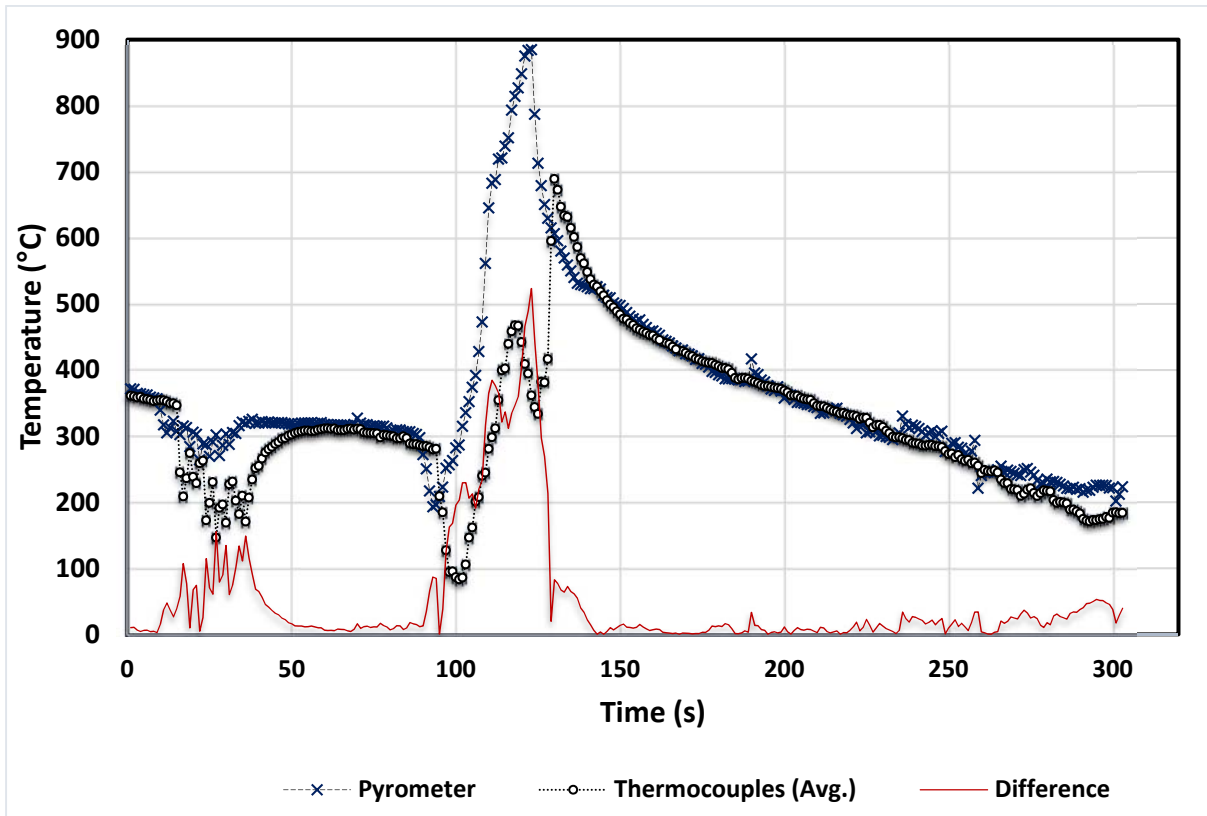


Figure 9. Comparison of Surface Temperatures of Smoldering Firebrands (Wind at 2-m/s)

The T620 FLIR[®] thermal camera was used to measure the surface temperature of smoldering firebrands. The emissivity was set to be 0.97 according to the emissivity results obtained in the previous section. An IR image was captured every 10-s until either the firebrand’s surface temperature dropped below 250°C, or it was blown away with wind, respectively. Three replicates for each experiment were used. Figure 11 shows a recorded frame at 6-m/s wind condition.

Using the FLIR ResearchIR[®] software, a bounding box was created around the firebrand at each frame and temperature values in every single pixel of the frame were recorded. Since firebrands burn non-uniformly, and the critical surface temperature of wood is 250-300°C, a MATLAB[®] code was developed to eliminate any pixel with a temperature value lower than 300°C, the ignition temperature of wood. Regarding the IR camera calibration range, authors chose the range that fits the measurement needs the best.

Then, after removing pixels with Temperature < 300°C, the average (of remaining pixels) temperature was calculated and plotted in Figure 12. The error bars represent one standard deviation of three measurements performed at each time interval. For these experiments the top surface temperature of firebrands ranged from 300°C to 1000°C depending on the wind speed.

Results showed that higher wind speed resulted in higher surface temperature on the whole surface of structural firebrands. Moreover, the average surface temperature in presence of wind remained almost steady during the test. With no wind the temperature decreased by 200°C in 400 seconds.

Fire Ember Production from Wildland and Structural Fuels

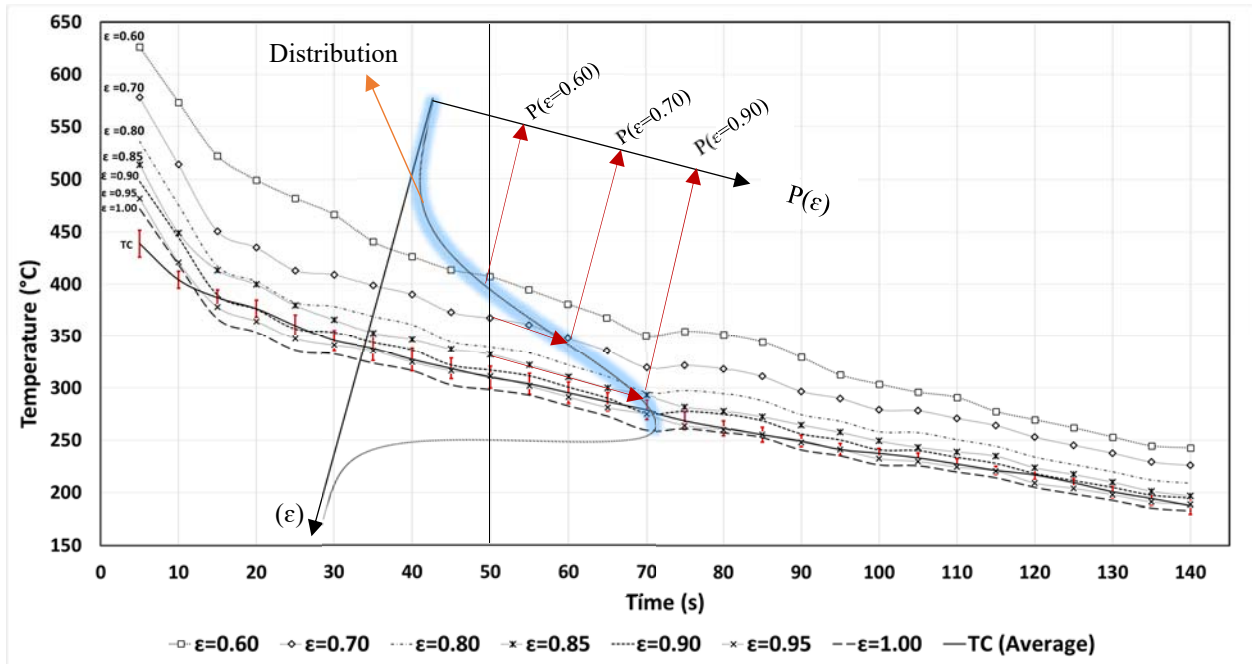


Figure 10. Temperature Variation and the probability of matching the thermocouple measurements at Different Emissivity Values.

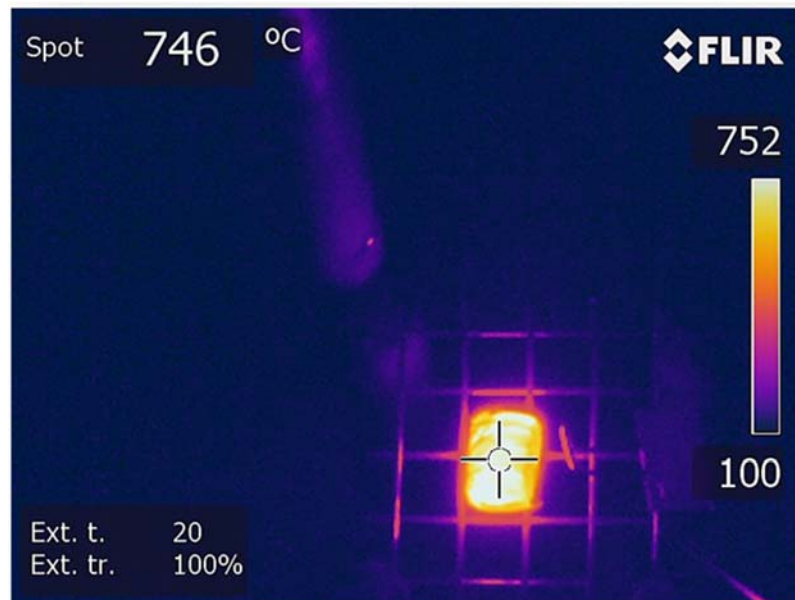


Figure 11. A Sample IR Image from 6-m/s Wind Test

Fire Ember Production from Wildland and Structural Fuels

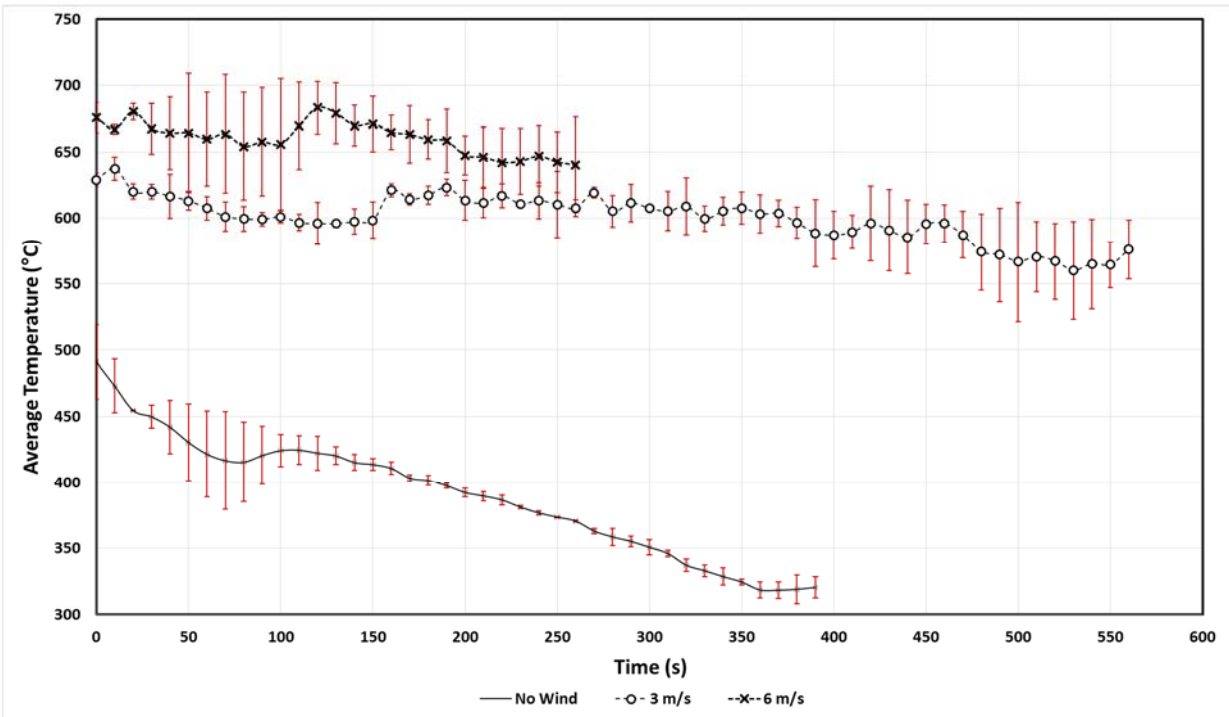


Figure 12. Average Temperature of the Pixels with $T > 300^{\circ}\text{C}$

The maximum surface temperature of a firebrand can assess the ignition potential of firebrands. As shown in Figure 13, firebrands could reach the temperature of 1000°C , and mostly fluctuating around 900°C in 6-m/s wind. On the other hand, medium wind speed used in this study could be considered as the most hazardous one. At the highest wind speed, firebrands rapidly lost mass and burned out in less than 300-s, but firebrands' smoldering continues for a longer period (600-s) at a smaller mass loss rate and steady temperature ($\sim 800^{\circ}\text{C}$) in medium wind speed. Considering Figures 12 and 13, one might interpret that at the medium wind speed, the magnitude of the generated heat for the firebrand is larger than that of at high wind speed.

These experiments show the surface temperature of the firebrands are not uniform. Figure 14 depicts the variation in the area with specific surface temperatures. The surface temperature of the firebrands is divided into four bins and plotted at 100 seconds intervals; the 10th second, the 110th second, and the 210th second of the experiment. In the top section of Figure 14, the first photo in each row shows the entire fire brand at the beginning, middle and towards the end of the experiment. The following images in each row shows the area with specific temperature range on the surface. The original firebrand size prior to ignition was 625 mm^2 which was slightly reduced to 559 mm^2 after flaming out. The bar charts at the bottom section of the Figure 14 shows the percentage of each temperature bin from the entire firebrand. A general observation is that the surface area with higher temperature increases with time until burn out.

Fire Ember Production from Wildland and Structural Fuels

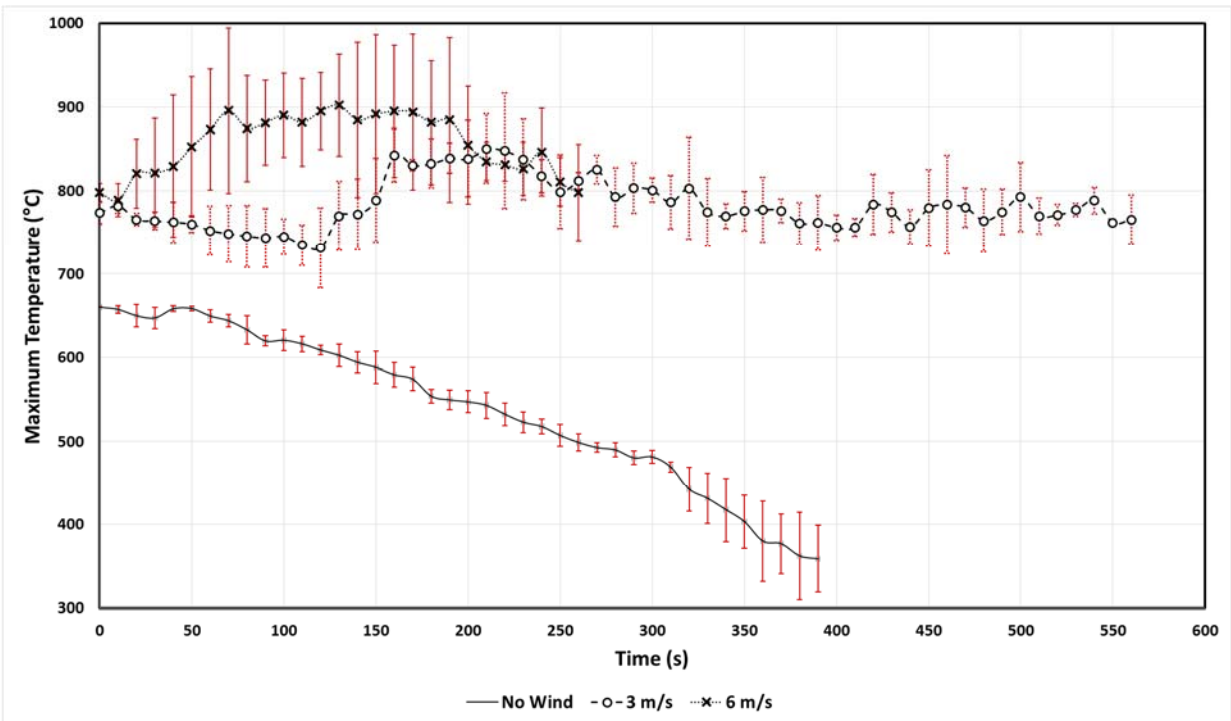


Figure 13. Maximum Temperature of Smoldering Firebrands

The response time of thermocouples limited their ability to record temperatures when wind caused the sudden increase of the firebrand's surface temperature. Moreover, at high wind speeds, the thermocouple tip lost its thermal equilibrium with the surface. However, optical devices can overcome these problems, and are the preferred to measure the surface temperature of a smoldering firebrand. Among many factors affecting the accuracy of an IR device's recording, the radiative emissivity (ϵ) value is the most influential parameter, which needs to be set accurately for each measurement. Experiments followed by a statistical analysis showed that the emissivity value for IR cameras in the spectral range of 7.5-14 μ m is in the range of 0.91 to 1.00 with 99% confidence. Choosing the emissivity value of 0.97, it was observed that the surface temperature of the smoldering firebrand varied from 300°C to 1000°C in different wind speeds.

Fire Ember Production from Wildland and Structural Fuels

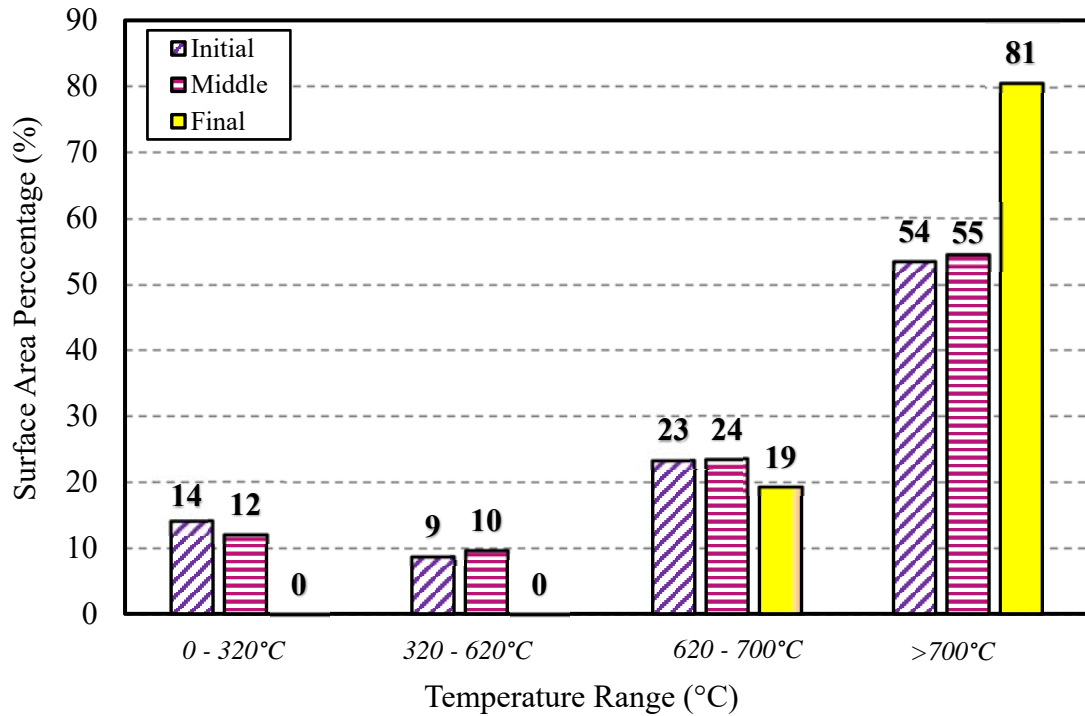
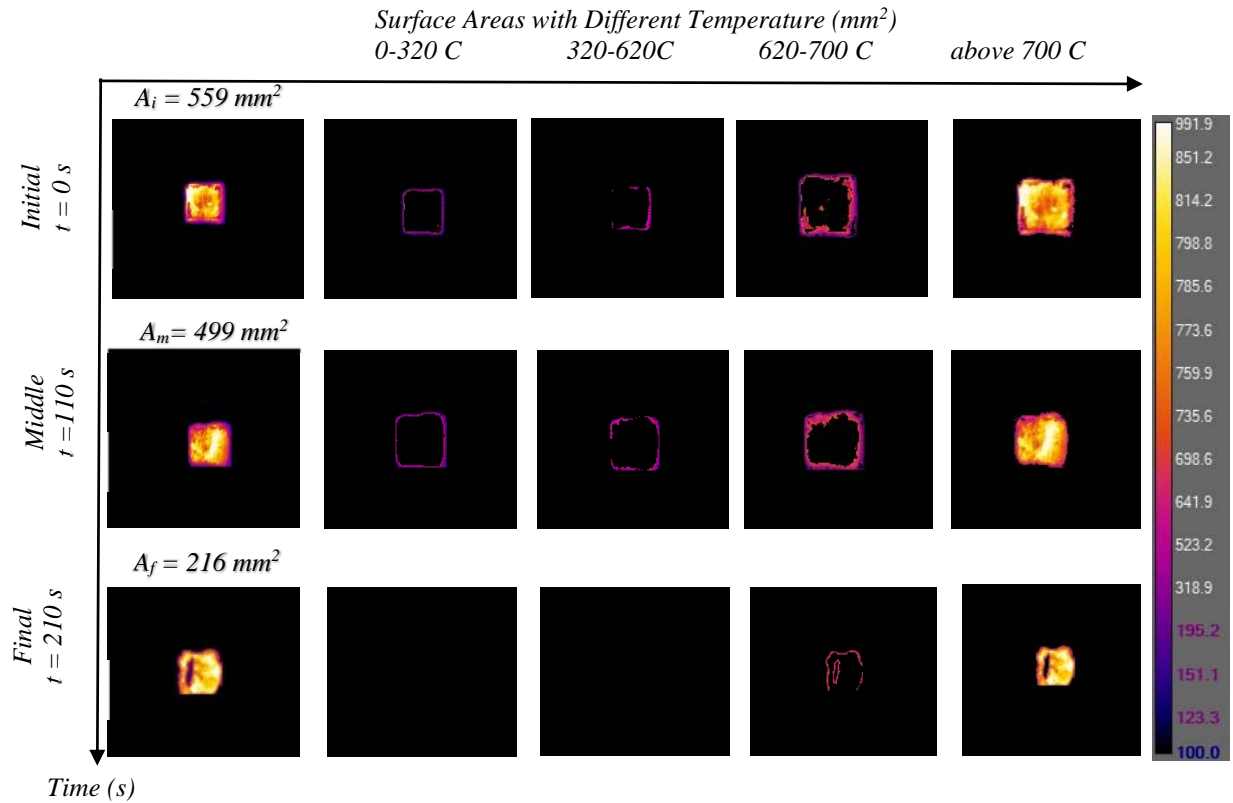


Figure 14. Results of infrared camera of a smoldering firebrand with initial size of 2.5-cm \times 2.5-cm and wind flow of 3-m/s.

5. Discussion

In this research project, we determined the basic thermal decomposition and combustion properties of selected fuels (at small-scale) under a range of heating rate, radiant heat flux, and MC levels. We also determined the mass, size, and flying distance of embers (at full-scale) from burning wildland and structural fuels under a range of wind speeds. The burning duration and intensity of embers under a range of wind conditions was also investigated.

5.1 Effect of MC Levels on Pyrolysis and Combustion Properties of Structural Fuels

The pyrolysis and combustion properties of seven representative structural fuels as a function of fuel MC levels under various external heating conditions were measured. The pyrolysis properties were measured using TGA at three MC levels (5, 10, and 15%) and three heating rates (5, 15, and 25 K/min.). The combustion properties were measured using a Cone Calorimeter at the same MC levels and three heat flux levels (20, 30, and 50kW/m²). In addition, density and thermal conductivity as a function of MC levels were also measured. Statistical analysis was performed over the experimental data using a 95% confidence interval. Most materials had significant increase in density when the MC levels increased, while the increase was more significant for natural woods than engineered woods. No statistically significant changes in thermal conductivity were observed for most materials. The pyrolysis properties were affected by both the MC and heating rate levels. Both MC and heat flux levels affected the combustion properties.

5.2 Effect of Wind Speed on Firebrand Production and Firebrand Intensity

Full-scale experiments were conducted to generate firebrands from burning structure assemblies in a boundary layer wind tunnel. A process for efficiently measuring traveling distance and project area was employed for a large sample size. An image processing algorithm was developed to measuring project area of each firebrand in batches. The projected area accompanied with traveling distance and wind speed was used to train a predictive model for estimating the mass of individual firebrands. The comparison between the predicted mass and measured mass shows a maximum error of 5%, confirming the accuracy of the model. This framework provides a methodology for efficiently measuring travel distance and project area along with a model that provides a probabilistic range for the estimation of firebrand mass/projected area/flying distance. Using this method for future testing will reduce the resource demands for measuring large sample sizes and reliably characterizing firebrands. 59,820 firebrands were collected and measured, with 24,149 from structural assemblies (fences, re-entrant corners, and roofs), 26,422 from wall-roof mockup structural assemblies, and 9,249 from five wildland vegetative fuels. The sample size of this study is significantly larger than any existing firebrand data sets. This work was based on a statistics-based framework for the sampling and measurement processes in firebrand generation experiments so that the obtained firebrand data can achieve the desired level of statistical reliability. These firebrand data sets are useful in understanding the characteristics and distribution of firebrands generated from various structural fuels. They can be used for developing and training predictive models for the firebrand phenomenon (generation, transport, and ignition), models to predict fire spread in the wildland and wildland-urban interface, and models to estimate risks from wildfire.

They are also useful for wildfire mitigation strategies or guidelines to minimize threat and damage from firebrand attacks.

Experiments on the burning duration and intensity of firebrands showed that wind played a critical role in the burning intensity of firebrands. It was observed that the emissivity of a smoldering firebrand varied between 0.91 and 1.00, with 99% confidence. Depending on the wind speed, the surface temperature of smoldering firebrands varied from 300 to 1000°C using $\epsilon=0.97$. It was also observed that only 50% of the firebrands' surfaces had temperatures greater than 700°C after flaming combustion ceased. In the presence of wind, this fraction gradually decreased to 25%. With no wind, however, it rapidly dropped to 10 % and lower wind speeds.

5.3 Impact of Firebrand Properties on Ignition Potential and Fire Spread in the WUI

One of the most complex and stochastic processes to understand in WUI fire spread is the ignition of recipient or "target" fuels by firebrands. Despite many years of study on the topic, it is not yet possible to formulate the ignition potential of fuels a priori based on both firebrand and target fuel properties. A framework for studying this phenomenon has appeared in the literature that takes account the known sensitivity of ignition time to firebrand size/mass and target fuel properties [2]. Several key properties affect the firebrand's impact on its ignition potential and fire spread in the WUI, such as its mass and size, thermal degradation and combustion properties, and subjected environmental conditions. Depending on these variables, an ignited recipient fuel may start glowing combustion and then die out, just smolder, or transition from smoldering to flaming and grow into a larger fire. Understanding the effects of each of the above variables on the ignition process is important in order to develop a physical model for firebrand ignition.

As part of this project, the ignition of polyurethane (PU) insulation foams subjected to firebrand attacks was investigated through experiments under controlled laboratory conditions [46,47]. The experimental study examined the effects of the following testing parameters on foam ignition probability: Flame-retardant (FR) treatment of recipient material (treated vs. non-treated), combustion mode of firebrand (flaming vs. smoldering), number of firebrand (single vs. ember piles), orientation of firebrand contact (top vs. side), and environmental wind. The foam ignition data were further analyzed using ANOVA and a machine learning procedure. This study showed that the probability of recipient fuel ignition under firebrand attack is affected by many factors. Among the five factors examined in the study, the top three factors are FR treatment of recipient fuel, combustion mode of firebrand, and the number of firebrands the foam is subjected to. Treated foam samples sufficiently inhibit ignition and flame. Ignition potential of foams exposed to single firebrand was significantly lower in comparison to multiple accumulated firebrands. Flaming firebrands in ambient conditions had a greater effect on ignition in comparison to smoldering firebrands in a similar condition. Environmental wind had some effect on ignition. Wind speeds lower than 3.5 m/s induced a greater chance for foam ignition whereas wind speeds greater than 3.5 m/s then reduced ignition chances. The firebrand/foam contact orientation (top vs. side) during test had the least impact on the probability of ignition. However, the firebrands placed on the side of the foam sample had a slightly greater but negligible effect on ignition than firebrands placed on top of the samples.

5.4 Implications of Results to Standards and Mitigation Related to Firebrand Attacks

The collected firebrands from previous firebrand production experiments using full-scale building components and their assemblies varied between 50 and 500 firebrands. The sample size of this study is significantly larger than any existing firebrand data sets. In addition, this work was based on a statistics-based framework for the sampling and measurement processes in firebrand generation experiments so that the obtained firebrand data can achieve the desired level of statistical reliability [35]. These firebrand data sets are useful in understanding the characteristics and distribution of firebrands generated from various structural fuels. They can be used for developing and training predictive models for the firebrand phenomenon (generation, transport, and ignition), models to predict fire spread in the wildland and wildland-urban interface, and models to estimate risks from wildfire. They can be useful for wildfire mitigation strategies or guidelines to minimize threat and damage from firebrand attacks. The results will also be useful for the engineering and standard/code organizations to develop standards or codes related to firebrands.

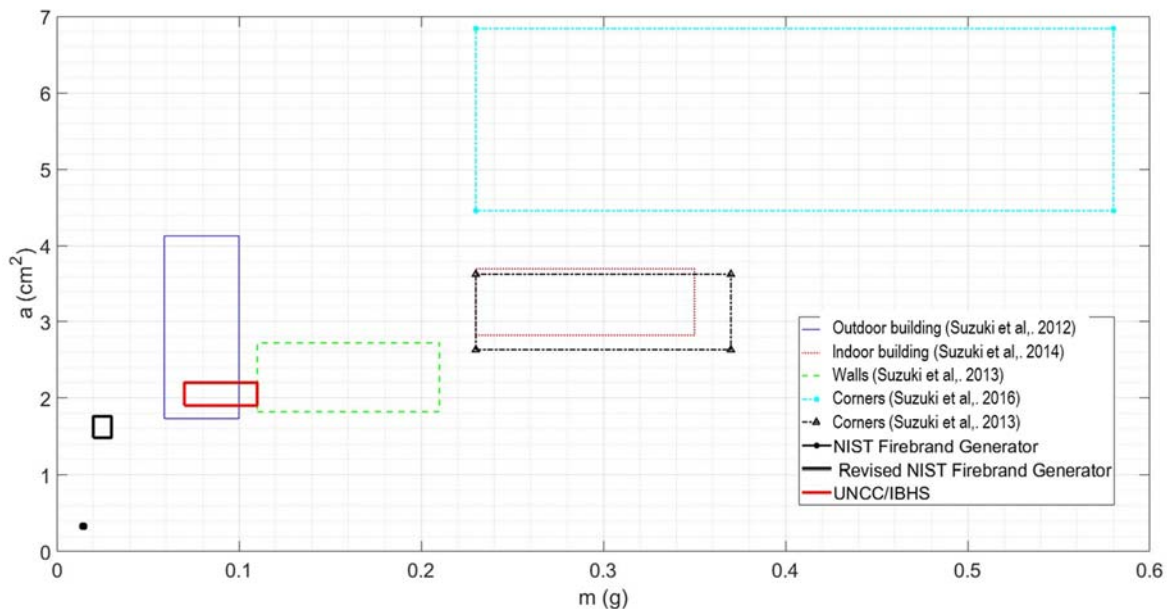


Figure 15. Comparison of Mass and Projected Area of Firebrands (95% Confidence Interval)

As an example [45, 48], Figure 15 compares the mass and projected area of firebrands from various studies under similar testing conditions (wind speed ~ 6 m/s, 95% confidence interval). One can observe that the firebrands generated from outdoor burns were lighter than those generated from indoor building and assembly burns. The ranges of firebrand mass and projected area from firebrand generators were much smaller than the firebrands generated from actual structural fuels (buildings or assemblies). Firebrands from first generation generators are so small that they only appear as a black dot in the left bottom corner in the figure (in the 0.01-0.02g and 0.2-0.4cm² cell). The firebrands generated from the revised firebrand generator are heavier and larger than that of from the first generation, which shows a significant improvement. It needs to be mentioned that the experiment procedures, sample materials, moisture contents etc. are different in some of these experiments which may affect the accuracy of the confidence intervals. However, this kind of comparison can help improve the design of firebrand generators and improve our understanding of mass and size of firebrands for standards and codes development.

5.5 Additional Analysis of Firebrand Data

This project generated a large amount of new firebrand data from full-scale firebrand production experiments under various gusty winds in a wind tunnel facility. The analysis as described in the report is basic using simple statistical analysis tools. Additional analysis of data using advanced statistical tools may lead to answers to more questions about firebrands. For example, more analysis should be performed to provide meaningful comparisons in firebrand size and mass by structural assembly types and vegetation species. Further correlation analysis should be performed to elucidate how assemblies or species and wind speed can affect the firebrand parameters.

An interesting question is “Can the distributions of firebrand parameters be modelled with known statistical distributions?”. As part of this project, structural firebrand data generated between the early 1960s and 2017 were compiled and analyzed in [45]. After plotting the histograms, the Maximum Likelihood Method was employed to find the best PDF candidates. Bayesian Information Criterion score was also calculated for each PDF. Results in [45] indicated Lognormal and Truncated Normal distributions provided the best overall modeling of firebrand parameters. Similar studies as described in Chapter 2 of [45] should be performed using these new firebrand data to provide more insight into the question.

Additional data analysis is underway by the research team to address these issues [49].

5.6 Implications for Future Research

The process of characterizing the physical properties of individual firebrands can be more tedious than conducting the tests. For a single experiment, the whole firebrand population is often extremely large. This makes the complete collection, enumeration, and characterization of the whole firebrand population impractical or impossible. Sampling techniques play a pivotal role in the validity of the measurements. In future firebrand production research, statistical sampling should be used so that a subset of manageable size can be used to represent the whole firebrand population. Our research reported in [35] provides a statistics-based framework to facilitate firebrand characterization. The framework incorporates a machine learning predictive model for the sampling and measurement processes so that the obtained firebrand data can achieve the desired level of statistical reliability with increased efficiency. Researcher should incorporate new development in imaging and video analysis, machine learning, and artificial intelligence into firebrand production research.

There is need for a framework which can be adapted to relatively realistic simulations of real wildland or WUI fires for firebrand related research. There are many potential fuel types, both structural (construction materials) and vegetative (wildland fuels), which may invariably generate different ember fluxes that should be studied and compared. Higher wind speeds have yet to be approached in order to create a more realistic WUI fire situation. Most experiments have been conducted with wind speeds up to 10 m/s and at constant wind speed, while actual wind are gusty and wind speeds in excess of 20 m/s are often observed during WUI fires. In the high wind scenario in this study, gusty wind speed averaged 18-m/s (40-mph), with 3-s gust peaks of 23-m/s during testing. Future firebrand production research should consider more realistic simulations of real wildland or WUI fire conditions, such as gusty wind and heating from nearby burning fuels. Controlling environmental conditions such as relative humidity and temperature during testing remains a challenge in a laboratory or wind tunnel.

Fire Ember Production from Wildland and Structural Fuels

Research should continue to collect and quantify firebrands from real and simulated fires, including different vegetation, structures, and environmental conditions. It remains a challenge to quantify the firebrand flux as well as surface temperature and heat flux of a smoldering firebrand real time during firebrand production experiments. Very limited research appears in the literature on the actual process of firebrand generation and how it relates to the materials which generate firebrands. If more understanding can be garnered from specific fuel types, perhaps these distributions can be better understood. New development and advanced algorithm in image and video analysis may be able to assist researchers to obtain these critical firebrand properties. Developing in modeling and simulation may lead to virtual numerical firebrand generators. These virtual firebrand generators can be integrated into models to investigate the lofting, transport and landing of firebrands, and subsequent ignition of recipient fuels by firebrands.

Literature Cited

1. Byram GM (1954) Atmospheric conditions related to blowup fires. Station Paper No.35, US Forest Service Southeast Forest Experiment Station. (Ashville, NC)
2. Caton, S.E., Hakes, R.S.P., Gollner, M.J., Gorham, D.J., and Zhou, A. (2017) A Review of Pathways for Building Fire Spread in the Wildland Urban Interface Part I: Exposure Conditions, *Fire Technology*, 53(3), 429–473. doi:<http://dx.doi.org/10.1007/s10694-016-0589-z>
3. Koo E, Pagni PJ, Weise DR, and Woycheese JP (2010) Firebrands and spotting ignition in large-scale fires. *International Journal of Wildland Fire* 19, 818-843.
4. Maranghides A and Mell W (2011) A case study of a community affected by the Witch and Guejito fires. *Fire Technology* 47, 379–420.
5. Quarles S, Leschak P, Cowger R, Worley K, Brown R., Iskovitz C (2012) Lessons learned from Waldo Canyon: Fire Adapted Communities Mitigation Assessment Team findings. IBHS. (Richburg, SC)
6. Manzello SL and Foote EID (2014) Characterizing firebrand exposure from wildland-urban interface (WUI) fires: Results from the 2007 Angora fire. *Fire Technology* 50, 105-124.
7. Albini, F.A. (1979) Spot Fire Distance from Burning Trees: A Predictive Model, USDA Forest Service, Intermountain Forest and Range Experiment Station, Technical Report INT-56, Ogden, UT, 1979, 73p.
8. Finney MA (2004) FARSITE: Fire area simulator – model development and evaluation. USDA Forest Service Rocky Mountain Research Station research paper RMRS-RP-4 revised. (Missoula, MT)
9. Andrews PL (2013) Current status and future needs of the BehavePlus fire modeling system. *International Journal of Wildland Fire* 23(1): 21-33.
10. Lautenberger C (2013) Wildland fire modeling with an Eulerian level set method and automated calibration. *Fire Safety Journal* 62: 289-298.
11. Mell WE (2013) USFS Fire models in use today. Unpublished webinar slides, June 6, 2013.
12. Tarifa CS, del Notario PP, Moreno FG, Villa AR (1967) Transport and combustion of firebrands. Instituto Nacional de Tecnica Aeroespacial, final report of Grants FG-SP-114 and FG-SP-146 (Vol. II). (Madrid, Spain)
13. Vodvarka F (1969) Firebrand field studies, Report J6148. IIT Research Institute. (Chicago, IL)
14. Waterman TE (1969) Experimental study of firebrand generation-report J6130. IIT Research Institute. (Chicago, IL)
15. Vodvarka FJ (1970) Urban Burns - Full-scale Field Studies, Technical Report J6171, IIT Research Institute, Chicago, IL, January 1970, 150 p.
16. Muraszew A (1974) Firebrand Phenomena, Report No. ATR-74(8165–01)-1, The Aerospace Corporation, El Segundo, CA, 1974, 117p.
17. Muraszew A, Fedele JB, Kuby WC (1975) Firebrand investigation. Aerospace Report No. ATR-75(7470)-1, the Aerospace Corporation. (El Segundo, CA)
18. Muraszew A, Fedele JB (1976) Statistical model for spot fire hazard. Aerospace Report No. ATR-77(7588)-1, the Aerospace Corporation. (El Segundo, CA)
19. Clements HB (1977) Lift-off of forest firebrands (Research Paper SE-159). USFS Southeastern Forest Experiment Station. (Asheville, NC)
20. Ellis PF (2000) The aerodynamic and combustion characteristics of eucalypt bark – a firebrand study. Ph.D. thesis, Australian National University. (Canberra, Australia)
21. Woycheese JP (2000) Brand lofting and propagation from large-scale fires. Ph.D. dissertation, the University of California at Berkeley. (Berkeley, CA)

22. Yoshioka H, Hayashi Y, Masuda H, Noguchi T (2004) Real-scale fire wind tunnel experiment on generation of firebrands from a house on fire. *Fire Science and Technology* 23(2): 142-150.
23. Manzello SL, Maranghides A, Mell WE (2007) Firebrand generation from burning vegetation. *International Journal of Wildland Fire* 16, 458–462.
24. Manzello SL, Shields JR, Cleary TG, et al. (2008) On the development and characterization of a firebrand generator. *Fire Safety Journal* 43: 258-268.
25. Manzello SL, Park S-H, Cleary TG (2009) Investigation on the ability of glowing firebrands deposited within crevices to ignite common building materials. *Fire Safety Journal* 44: 894-900.
26. Manzello SL, Maranghides A, Shields JR, et al. (2009) Mass and size distribution of firebrands generated from burning Korean pine (*Pinus koraiensis*) trees. *Fire and Materials* 33: 21-31.
27. Suzuki S, Manzello SL, Lage M, and Laing G (2012) Firebrand generation data obtained from a full-scale structure burn. *International Journal of Wildland Fire* 21, 961–968.
28. Manzello SL, Suzuki S (2013) Experimentally simulating wind driven firebrand showers in WUI fires: Overview of the NIST firebrand generator (NIST dragon) technology. *Procedia Engineering* 62: 91-102.
29. Suzuki S, Manzello SL, Lage M, Laing G (2012) Firebrand generation data obtained from a full-scale structure burn. *International Journal of Wildland Fire* 21: 961–968.
30. Suzuki S, Manzello SL, Hayashi Y (2013) The size and mass distribution of firebrands collected from ignited building components exposed to wind. *Proceedings of the Combustion Institute* 34: 2479-2485.
31. Suzuki S, Brown A, Manzello SL, Suzuki J, Hayashi Y (2014) Firebrands generated from a full-scale structure burning under well-controlled laboratory conditions. *Fire Safety Journal* 63: 43-51.
32. Zhou K, Suzuki S, Manzello SL (2014) Experimental study of firebrand transport. *Fire Technology*, in press.
33. Suzuki S, Manzello SL (2016) Firebrand production from building components fitted with siding treatments. *Fire Safety Journal* 80:64-70.
34. Manzello SL, Suzuki S (2017) Generating wind-driven firebrand showers characteristic of burning structures. *Proceedings of the Combustion Institute* 36 (2):3247-3252.
35. Hedayati, F., Bahrani, B., Zhou, A., Quarles, S.L., Gorham, D. (2019). A Framework to Facilitate Firebrand Characterization, *Frontiers in Mechanical Engineering - Thermal and Mass Transport*, 5(43), <https://doi.org/10.3389/fmech.2019.00043>
36. Hedayati F, Yang W, Zhou A. (2018) Effects of moisture content and heating condition on pyrolysis and combustion properties of structural fuels, *Fire and Materials*, 42:741–749. doi: <https://doi.org/10.1002/fam.2528>
37. Weise DR, White RH, Beall FC, Etlinger M (2005) Use of the cone calorimeter to detect seasonal differences in selected combustion characteristics of ornamental vegetation. *International Journal of Wildland Fire*, 14:321-338.
38. Overholt KJ, Cabrera J, Kurzwaski A, Koopersmith M, Ezekoye OA (2014) Characterization of fuel properties and fire spread rates for little bluestem grass. *Fire Technology* 50: 9-38.
39. ASTM D4442-15, Standard Test Methods for Direct Moisture Content Measurement of Wood and Wood-Based Materials, ASTM International, West Conshohocken, PA, 2015.
40. ASTM D2395-14e1 Standard Test Methods for Density and Specific Gravity (Relative Density) of Wood and Wood-Based Materials, ASTM International, West Conshohocken, PA, 2014.

41. ASTM C518-17, Standard Test Method for Steady-State Thermal Transmission Properties by Means of the Heat Flow Meter Apparatus, ASTM International, West Conshohocken, PA, 2017.
42. ASTM E1354-14, Standard test method for heat and visible smoke release rates for materials and products using an oxygen consumption calorimeter, ASTM Int., West Conshohocken, PA, 2014.
43. Yang W. (2016) Pyrolysis and combustion properties of selected structural fuels in residential buildings, MS Thesis, University of North Carolina at Charlotte, Charlotte, NC. Online access: <https://ninercommons.uncc.edu/islandora/object/etd%3A1637>.
44. Hamann E, Bahrani B, Kadel J, Stickles M, Zhou A. (2017). Ignition of attic insulation foams subjected to firebrands. Proceedings of the 15th International Conference on Fire and Materials, 6-8 February 2017, San Francisco, CA.
45. Hedayati F (2018) Generation and characterization of firebrands from selected structural fuels. PhD Dissertation. University of North Carolina at Charlotte, Charlotte, NC. Online access: <https://repository.uncc.edu/islandora/object/etd%3A986>.
46. Hamann E, Bahrani B, Kadel J, Stickles M, Zhou A (2017) Ignition of attic insulation foams subjected to firebrands, Proceedings of the 15th International Conference on Fire and Materials, 6 - 8 February 2017, San Francisco, USA, p727-739.
47. Zhou A. (2018) Ignition of polyurethane insulation foam subjected to burning firebrands, Technical Report, Department of Engineering Technology and Construction Management University of North Carolina at Charlotte, Charlotte, NC, USA. p. 25.
48. Zhou A and Quarles SL. (2018) Characterization of firebrands from common structural and wildland vegetative fuels, Fire Continuum Conference, Missoula, MT, May 21-24, 2018.
49. Bahrani B and Zhou A. (2019) Characteristics of Firebrands from Selected Vegetative Fuels, SFPE 2019 Annual Conference and Expo, Phoenix, AZ, October 13-15, 2019.

Appendix A: Contact Information for Key Project Personnel

Principal Investigator:

Aixi Zhou, Ph.D., P.E., Professor and Chairperson
 Department of Applied Engineering Technology
 College of Science and Technology | Price Hall, Suite 100
 North Carolina A&T State University
 1601 East Market Street, Greensboro, NC 27411
 Phone: (336) 285-3158; Fax: (336) 334-7704
 Email: azhou@ncat.edu

Co-Principal Investigator

Stephen L. Quarles, Ph.D., Chief Scientist (Retired) /Consultant
 Insurance Institute for Business & Home Safety
 5335 Richburg Road, Richburg, SC 29729
 Phone: (813) 404-4942; Cell: (415) 233-1141
 Email: squarles@ibhs.org

Funding Cooperator and Collaborator

David R. Weise, Ph.D., Research Forester
 Forest Service Pacific Southwest Research Station
 4955 Canyon Crest Drive, Riverside, CA 92507
 Phone: 951-680-1543; Cell: 951-236-4886; Fax: 951-680-1501
 Email: david.weise@usda.gov

The following table lists the roles of investigators and associated personnel in this project.

Personnel	Role	Responsibility
Aixi Zhou (UNCC and N.C. A&T)*	PI	Overall project responsibility
Stephen L. Quarles (IBHS)**	Co-PI	Ember production and characterization experiments
David R. Weise (PSW Research Station)	Funding Cooperator and Collaborator	Chamise collection; project agreement with JFSP and team members; project data management at USFS
Ofodike A. Ezekoye (U. of TX)	Collaborator	Texas prairie grass (little bluestem grass) collection
Michael J. Gollner (U. of MD)	Collaborator	Role of ember production and characteristics in WUI fire spread
Casey Grant (NFPA-FPRF)	Collaborator	Knowledge transfer to NFPA, Firewise communities, and others
Alan J Long (U. of FL, JFSP-SFE)	Contributor	Science delivery in the fire management community.

*: Dr. Aixi Zhou moved to N.C. A&T in August 2018.

** Dr. Stephen Quarles retired from IBHS in August 2018.

Appendix B: List of Delivery Products

Journal Articles

1. Hedayati F, Bahrani B, Zhou A, Quarles SL, Gorham D. (2019). A framework to facilitate firebrand characterization, *Frontiers in Mechanical Engineering - Thermal and Mass Transport*, Vol. 5, Article 43, <https://doi.org/10.3389/fmech.2019.00043>.
2. Caton-Kerr SE, Tohidi A, Gollner MJ (2019) Firebrand Generation from Thermally-Degraded Cylindrical Wooden Dowels, *Frontiers in Mechanical Engineering*, 5:32. <https://doi.org/10.3389/fmech.2019.00032>.
3. Wessies S, Chang R, Marr KC, Ezekoye OA. (2019) Experimental and Analytical Characterization of Firebrand Ignition of Home Insulation Materials, *Fire Technology*, <https://link.springer.com/article/10.1007/s10694-019-00818-8>
4. Hedayati F, Yang W, Zhou A. (2018) Effects of moisture content and heating condition on pyrolysis and combustion properties of structural fuels, *Fire and Materials*, 42:741–749.
5. Hakes R, Caton S, Gorham DJ, Zhou A, Gollner MJ (2017) Pathways to Fire Spread in the Wildland Urban Interface Part I: Exposure conditions, *Fire Technology*, 53(2), 429–473.
6. Hakes R, Caton S, Gorham DJ, Gollner MJ. (2017) Pathways to Fire Spread in the Wildland Urban Interface Part II: Response of Components and Systems and Mitigation Strategies, *Fire Technology*, 53(2), 475–515.

Thesis and Dissertation

1. Yang W. (2016) Pyrolysis and Combustion properties of selected structural fuels in residential buildings, MS Thesis, University of North Carolina at Charlotte, Charlotte, NC. Online access: <https://ninercommons.uncc.edu/islandora/object/etd%3A1637>.
2. Hedayati F (2018) Generation and characterization of firebrands from selected structural fuels. PhD Dissertation. University of North Carolina at Charlotte, Charlotte, NC. Online access: <https://repository.uncc.edu/islandora/object/etd%3A986>.
3. Bahrani B. (2019) Generation and characterization of firebrands from selected vegetative fuels in wildfires. PhD Dissertation. University of North Carolina at Charlotte, Charlotte, NC. (To be published in Fall 2019).

Conference Proceedings

1. Wessies S, Marr KC, Ezekoye OA. (2019) Heat transfer characterization of a hot cylinder on an inert substrate, 4th Thermal and Fluids Engineering Conference (TFEC) – American Soc Thermal Fluids Engineers, Begel House Inc., 2019.
2. Hamann E, Bahrani B, Kadel J, Stickles M, Zhou A (2017) Ignition of attic insulation foams subjected to firebrands, *Proceedings of the 15th International Conference on Fire and Materials*, 6 - 8 February 2017, San Francisco, USA, p727-739.
3. Hedayati F, Zhou A (2017) Statistical analysis on firebrand generation from structural fuels, *Proceedings of the 15th International Conference on Fire and Materials*, 6 - 8 February 2017, San Francisco, USA, p.656-667.
4. Tohidi A, Caton S, Gollner MJ, Bryner N. (2017) Thermo-Mechanical Breakage Mechanism of Firebrands, 10th U. S. National Combustion Meeting, College Park, MD, April 23-26, 2017.

Conference Presentations (slides only, no proceedings)

1. Bahrani B and Zhou A. (2019) Characteristics of Firebrands from Selected Vegetative Fuels, SFPE 2019 Annual Conference and Expo, Phoenix, AZ, October 13-15, 2019.
2. Quarles SL and Zhou A. (2018) Wildland and WUI firebrand production, experimental data collection, 2018 NFPA Conference & Expo, June 11-14, 2018, Las Vegas, NV.
3. Quarles SL and Zhou A. (2018) Wildfire exposure to buildings: vulnerabilities and mitigation strategies, Fire Continuum Conference, Missoula, MT, May 21-24, 2018.
4. Zhou A and Quarles SL. (2018) Characterization of firebrands from common structural and wildland vegetative fuels, Fire Continuum Conference, Missoula, MT, May 21-24, 2018.
5. Wessies S, Marr KC, Ezekoye OA. (2018) Firebrand Ignition of Attic Insulation and an Ornamental Grass, Fire Continuum Conference Missoula, MT, May 2018.
6. Hedayati F and Zhou A. (2016). Statistical analysis on firebrand generation from structural fuels, SFPE 2016 North America Conference and Expo, Denver, CO, September 25-30, 2016.

Other Publications

1. Zhou A. (2018) Ignition of Polyurethane Insulation Foam Subjected to Burning Firebrands, Technical Report, Department of Engineering Technology and Construction Management University of North Carolina at Charlotte, Charlotte, NC, USA. p. 25.
2. Hedayati F, Bahrani B, Zhou A, Quarles SL, Weise DR. (2019). Data for Firebrands Generated from Selected Structural Fuels: Joint Fire Science Program Project (15-1-04-4). Forest Service Research Data Archive, Fort Collins, CO. doi: TBD
3. Bahrani B, Hedayati F, Zhou A, Quarles SL, Weise DR. (2019). Data for Firebrands Generated from Selected Vegetative Fuels: Joint Fire Science Program Project (15-1-04-4). Forest Service Research Data Archive, Fort Collins, CO. doi: TBD

Appendix C: Metadata

This project generated a large amount of new data from small-scale thermal degradation and combustion experiments and full-scale firebrand production experiments. Data and accompanying metadata for small-scale thermal degradation and combustion experiments are presented in References [36] and [43]. Full-scale firebrand production experiments were conducted in IBHS Research Center wind tunnel in Richburg, SC. Only firebrands with all three measurements (mass, projected area, and traveling distance) were recorded and reported. Three physical quantities of interests were measured and recorded. Traveling (or flying) distance, projected area and mass. Unites for these properties are projected area in cm^2 or mm^2 , mass in grams, traveling distance in meters. Flying distance was calculated based on the location of the pans with respect to the burning sample using the Pythagorean Theorem. To measure the projected area, an image processing algorithm was developed which automatically detects the edges of the background sheet, rotates the photo if its tilted before cropping, detects edges of firebrands, removes erroneous particles (e.g., ash) and finally calculates the projected area. For mass, the firebrands were placed on a high-precision digital balance (Sartorius H51, resolution of ± 0.0001 gram). Uncertainty for each variable is listed below: Mass: 0.0169-grams, Projected area: 0.09- mm^2 , Flying distance: 0.22-m. The firebrand data and accompanying metadata will be archived in the Forest Service Research Data Archive upon publication of peer-reviewed articles presenting the data.

Appendix D: Digital Images for Collected Firebrands

This project generated several hundred digital images for collected firebrands. Some selected images are shown in this appendix.

D.1 Digital Images for Collected Firebrands from Structural Fuels



(a) Corner_Cedar-OSB_High



(b) Corner_Cedar-Plywood_Medium

Figure 16. Representative Digital Images for Firebrands: Corner Assemblies



(a) Fence_Lattice_Idle Wind



(b) Fence_Privacy_High Wind

Figure 17. Representative Digital Images for Firebrands: Fences

Fire Ember Production from Wildland and Structural Fuels



(a) Roof_FRT Shake_High Wind



(b) Roof_Non-FRT Shake_High Wind

Figure 18. Representative Digital Images for Firebrands: Roofs

D.1 Digital Images for Collected Firebrands from Vegetative Fuels



Chamise_High Wind



Saw palmetto_High Wind

Figure 19. Representative Digital Images for Firebrands: Chamise and saw palmetto

Fire Ember Production from Wildland and Structural Fuels

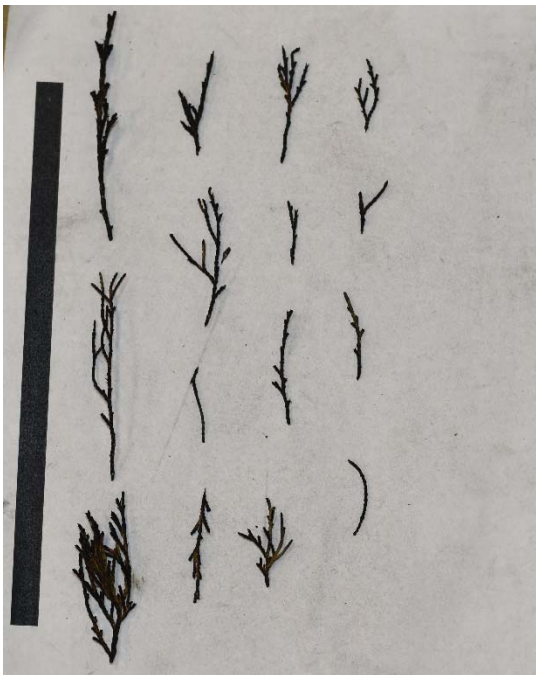


Loblolly pine_Idle Wind



Little Bluestem Grass_High Wind

Figure 20. Representative Digital Images for Firebrands: Southern Yellow Pine and Little Bluestem Grass



Leyland Cypress_Green_High Wind



Leyland Cypress_Dry_High Wind

Figure 21. Representative Digital Images for Firebrands: Green and Dry Layland Cypress

Appendix E: Statistical Results for Collected Firebrands

This project collected and measured the physical properties (mass, size and flying distance) of 59,820 firebrands: 24,149 from structural assemblies (fences, re-entrant corners, and roofs), 26,422 from wall-roof mockup structural assemblies, and 9,249 from five wildland vegetative fuels (chamise, saw palmetto, loblolly pine, Leyland cypress s, and little bluestem grass). The statistical results for these firebrands are provided in the appendix.

E.1 Statistical Results for Collected Firebrands from Structural Fuels

Table 4. Firebrand Parameters for Privacy Fence

Physical Quantity	Statistical Quantity	Constant Wind	Variable Wind (Avg. & Gust Peak)	
		Idle (5.36-m/s)	Medium (11.17 & 14.30-m/s)	High (17.88 and 23.00-m/s)
Flying Distance (m)	Mean	1.17	1.63	3.13
	Standard Deviation	0.73	1.78	3.11
	Skewness	2.17	3.30	1.61
	Median	0.94	0.94	1.69
Projected Area (cm ²)	Mean	6.92	4.83	3.08
	Standard Deviation	19.07	13.90	9.92
	Skewness	6.08	6.82	9.06
	Median	1.81	0.99	0.94
Mass (g)	Mean	1.06	0.61	0.27
	Standard Deviation	6.03	4.46	1.48
	Skewness	8.63	19.98	8.26
	Median	0.04	0.02	0.02
Correlation (r)	Mass and Area	0.92	0.80	0.94
	Mass and Flying Distance	-0.12	-0.04	-0.04
	Area and Flying Distance	-0.24	-0.09	-0.05
Sample Size		351	776	300

Fire Ember Production from Wildland and Structural Fuels

Table 5. Firebrand Parameters for Lattice Fence

Physical Quantity	Statistical Quantity	Constant Wind	Variable Wind (Avg. & Gust Peak)	
		Idle (5.36-m/s)	Medium (11.17 & 14.30- m/s)	High (17.88 and 23.00-m/s)
Flying Distance (m)	Mean	1.30	1.95	3.04
	Standard Deviation	1.85	3.72	2.89
	Skewness	4.07	5.34	1.39
	Median	0.72	0.84	1.69
Projected Area (cm ²)	Mean	3.02	1.94	2.51
	Standard Deviation	4.27	3.69	5.79
	Skewness	2.67	5.28	5.48
	Median	1.26	0.84	0.83
Mass (g)	Mean	0.21	0.11	0.29
	Standard Deviation	0.56	0.47	1.25
	Skewness	7.12	11.25	7.79
	Median	0.03	0.014	0.03
Correlation (r)	Mass and Area	0.82	0.88	0.95
	Mass and Flying Distance	-0.14	-0.11	-0.17
	Area and Flying Distance	-0.23	-0.19	-0.23
Sample Size		777	742	252

Fire Ember Production from Wildland and Structural Fuels

Table 6. Firebrand Parameters for Cedar Siding/Plywood Sheathing Corner Assemblies

Physical Quantity	Statistical Quantity	Constant Wind	Variable Wind (Avg. & Gust Peak)	
		Idle (5.36-m/s)	Medium (11.17 & 14.30- m/s)	High (17.88 and 23.00-m/s)
Flying Distance (m)	Mean	2.26	2.15	2.64
	Standard Deviation	2.73	2.08	3.34
	Skewness	2.47	1.98	1.97
	Median	1.29	1.42	1.16
Projected Area (cm ²)	Mean	3.97	3.75	4.64
	Standard Deviation	6.73	4.650	9.58
	Skewness	5.24	3.61	19.61
	Median	2.09	2.24	3.02
Mass (g)	Mean	0.31	0.21	0.30
	Standard Deviation	0.97	0.39	0.91
	Skewness	9.05	4.85	16.37
	Median	0.07	0.08	0.15
Correlation (r)	Mass and Area	0.81	0.81	0.78
	Mass and Flying Distance	0.82	-0.14	-0.21
	Area and Flying Distance	-0.14	-0.20	-0.21
Sample Size		1595	1435	1442

Fire Ember Production from Wildland and Structural Fuels

Table 7. Firebrand Parameters for Cedar Siding/OSB Sheathing Corner Assemblies

Physical Quantity	Statistical Quantity	Constant Wind	Variable Wind (Avg. & Gust Peak)	
		Idle (5.36-m/s)	Medium (11.17 & 14.30- m/s)	High (17.88 and 23.00-m/s)
Flying Distance (m)	Mean	2.71	3.20	5.07
	Standard Deviation	3.72	3.24	3.88
	Skewness	0.47	0.52	0.27
	Median	1.11	1.99	3.20
Projected Area (cm ²)	Mean	2.10	3.90	4.87
	Standard Deviation	2.72	6.48	7.87
	Skewness	5.17	6.62	13.47
	Median	1.26	2.08	2.99
Mass (g)	Mean	0.09	0.25	0.38
	Standard Deviation	0.24	1.28	1.44
	Skewness	7.63	25.37	21.99
	Median	0.02	0.06	0.14
Correlation (r)	Mass and Area	0.83	0.72	0.90
	Mass and Flying Distance	-0.20	-0.11	-0.07
	Area and Flying Distance	-0.24	-0.20	-0.10
Sample Size		1495	1400	1478

Fire Ember Production from Wildland and Structural Fuels

Table 8. Firebrand Parameters for OSB Siding/OSB Sheathing Corner Assemblies

Physical Quantity	Statistical Quantity	Constant Wind	Variable Wind (Avg. & Gust Peak)	
		Idle (5.36-m/s)	Medium (11.17 & 14.30- m/s)	High (17.88 and 23.00-m/s)
Flying Distance (m)	Mean	8.24	9.20	13.55
	Standard Deviation	8.84	10.79	11.20
	Skewness	1.63	1.55	0.72
	Median	5.10	5.10	8.05
Projected Area (cm ²)	Mean	1.28	2.97	5.27
	Standard Deviation	1.64	3.55	6.35
	Skewness	6.90	4.73	5.09
	Median	0.85	1.90	3.47
Mass (g)	Mean	0.05	0.18	0.55
	Standard Deviation	0.19	0.40	1.31
	Skewness	17.15	6.30	16.38
	Median	0.01	0.06	0.23
Correlation (r)	Mass and Area	0.86	0.91	0.89
	Mass and Flying Distance	-0.16	-0.19	-0.20
	Area and Flying Distance	-0.27	-0.22	-0.30
Sample Size		940	1400	1744

Fire Ember Production from Wildland and Structural Fuels

Table 9. Firebrand Parameters for Recycled Shake Roof Assemblies

Physical Quantity	Statistical Quantity	Constant Wind	Variable Wind (Avg. & Gust Peak)	
		Idle (5.36-m/s)	Medium (11.17 & 14.30- m/s)	High (17.88 and 23.00-m/s)
Flying Distance (m)	Mean	3.97	2.77	9.36
	Standard Deviation	3.95	2.80	7.19
	Skewness	2.75	1.86	1.15
	Median	2.2	0.75	6.55
Projected Area (cm ²)	Mean	3.50	3.05	2.92
	Standard Deviation	9.55	5.97	3.59
	Skewness	13.13	19.61	5.01
	Median	1.35	1.73	1.89
Mass (g)	Mean	0.43	0.30	0.22
	Standard Deviation	2.75	2.29	0.54
	Skewness	19.03	33.72	7.70
	Median	0.04	0.07	0.08
Correlation (r)	Mass and Area	0.95	0.91	0.92
	Mass and Flying Distance	-0.11	-0.06	-0.11
	Area and Flying Distance	-0.21	-0.14	-0.12
Sample Size		743	1401	1401

Fire Ember Production from Wildland and Structural Fuels

Table 10. Firebrand Parameters for FRT Cedar Shake Roof/OSB Sheathing Assemblies

Physical Quantity	Statistical Quantity	Constant Wind	Variable Wind (Avg. & Gust Peak)	
		Idle (5.36-m/s)	Medium (11.17 & 14.30- m/s)	High (17.88 and 23.00-m/s)
Flying Distance (m)	Mean	1.83	1.59	4.47
	Standard Deviation	2.08	1.75	3.99
	Skewness	2.91	3.41	1.16
	Median	0.94	0.74	2.54
Projected Area (cm ²)	Mean	6.75	7.41	5.73
	Standard Deviation	10.62	10.84	20.96
	Skewness	5.65	5.19	17.74
	Median	3.27	4.33	2.691
Mass (g)	Mean	0.67	0.81	0.71
	Standard Deviation	1.73	2.06	6.86
	Skewness	8.51	8.25	21.72
	Median	0.12	0.26	0.11
Correlation (r)	Mass and Area	0.87	0.87	0.95
	Mass and Flying Distance	-0.21	-0.20	-0.18
	Area and Flying Distance	-0.29	-0.28	-0.26
Sample Size		623	1401	1455

Fire Ember Production from Wildland and Structural Fuels

Table 11. Firebrand Parameters for Non-FRT Cedar Shake Roof/OSB Sheathing Assemblies

Physical Quantity	Statistical Quantity	Constant Wind	Variable Wind (Avg. & Gust Peak)	
		Idle (5.36-m/s)	Medium (11.17 & 14.30- m/s)	High (17.88 and 23.00-m/s)
Flying Distance (m)	Mean	6.13	7.69	12.98
	Standard Deviation	5.18	8.78	11.87
	Skewness	1.57	1.92	1.19
	Median	5.10	5.10	8.05
Projected Area (cm ²)	Mean	4.37	5.28	6.84
	Standard Deviation	10.47	11.77	16.95
	Skewness	6.52	9.14	10.95
	Median	1.04	2.08	3.75
Mass (g)	Mean	0.52	0.48	0.81
	Standard Deviation	2.59	1.87	4.95
	Skewness	11.52	9.72	12.76
	Median	0.02	0.07	0.17
Correlation (r)	Mass and Area	0.86	0.90	0.85
	Mass and Flying Distance	-0.17	-0.12	-0.08
	Area and Flying Distance	-0.29	-0.13	-0.06
Sample Size		1001	1430	1390

Fire Ember Production from Wildland and Structural Fuels

Table 12. Firebrand Parameters for Wall-Roof Mockups: Wood Cladding Only, Combustible Roof

Physical Quantity	Statistical Quantity	Idle (5.36-m/s)	Medium Wind (11.17-m/s)	High Wind (17.88-m/s)
Flying Distance (m)	Mean	4.203	6.928	5.408
	Standard Deviation	4.315	6.118	7.198
	Skewness	1.162	0.606	1.385
	Median	2.028	5.128	1.684
Projected Area (cm ²)	Mean	2.434	2.079	3.779
	Standard Deviation	5.008	3.714	10.781
	Skewness	6.204	11.441	14.021
	Median	0.849	1.197	1.935
Mass (g)	Mean	0.184	0.120	0.350
	Standard Deviation	0.611	0.542	1.501
	Skewness	6.259	18.833	11.810
	Median	0.018	0.027	0.094
Mass and Area Correlation		0.871	0.928	0.900
Mass and Flying Distance Correlation		-0.240	-0.175	-0.111
Area and Flying Distance Correlation		-0.311	-0.308	-0.135
Sample Size		537	891	915

Fire Ember Production from Wildland and Structural Fuels

Table 13. Firebrand Parameters for Wall-Roof Mockups: Wood Cladding Only, Noncombustible Roof

Physical Quantity	Statistical Quantity	Idle (5.36-m/s)	Medium Wind (11.17-m/s)	High Wind (17.88-m/s)
Flying Distance (m)	Mean	2.786	3.994	5.691
	Standard Deviation	3.397	4.704	6.860
	Skewness	1.700	1.552	1.322
	Median	1.158	1.856	2.028
Projected Area (cm ²)	Mean	2.206	2.567	3.237
	Standard Deviation	2.227	3.440	6.216
	Skewness	2.418	5.228	11.279
	Median	1.495	1.571	1.971
Mass (g)	Mean	0.135	1.334	0.230
	Standard Deviation	0.270	33.540	0.675
	Skewness	4.370	28.525	10.392
	Median	0.046	0.050	0.079
Mass and Area Correlation		0.899	0.012	0.925
Mass and Flying Distance Correlation		-0.291	-0.023	-0.106
Area and Flying Distance Correlation		-0.422	-0.249	-0.117
Sample Size		497	814	1109

Fire Ember Production from Wildland and Structural Fuels

Table 14. Firebrand Parameters for Wall-Roof Mockups: Wood Cladding Assembly, Combustible Roof

Physical Quantity	Statistical Quantity	Idle (5.36-m/s)	Medium Wind (11.17-m/s)	High Wind (17.88-m/s)
Flying Distance (m)	Mean	3.003	6.828	6.640
	Standard Deviation	3.661	6.533	6.190
	Skewness	1.803	0.754	1.129
	Median	1.470	3.154	5.128
Projected Area (cm ²)	Mean	2.127	2.589	2.824
	Standard Deviation	2.573	4.299	7.752
	Skewness	4.297	7.788	14.414
	Median	1.441	1.466	1.285
Mass (g)	Mean	0.134	0.179	0.211
	Standard Deviation	0.336	0.642	1.118
	Skewness	10.004	12.384	19.509
	Median	0.043	0.042	0.049
Mass and Area Correlation		0.903	0.875	0.939
Mass and Flying Distance Correlation		-0.240	-0.186	-0.122
Area and Flying Distance Correlation		-0.384	-0.276	-0.174
Sample Size		690	1104	1035

Fire Ember Production from Wildland and Structural Fuels

Table 15. Firebrand Parameters for Wall-Roof Mockups: Wood Cladding Assembly, Noncombustible Roof

Physical Quantity	Statistical Quantity	Idle (5.36-m/s)	Medium Wind (11.17-m/s)	High Wind (17.88-m/s)
Flying Distance (m)	Mean	3.298	7.108	5.352
	Standard Deviation	3.622	6.281	5.699
	Skewness	1.452	0.601	1.007
	Median	1.684	5.128	2.646
Projected Area (cm ²)	Mean	2.259	2.463	3.026
	Standard Deviation	3.706	3.284	4.668
	Skewness	6.095	4.985	5.014
	Median	1.295	1.423	1.549
Mass (g)	Mean	0.151	0.156	0.242
	Standard Deviation	0.519	0.467	0.566
	Skewness	10.931	8.746	5.413
	Median	0.039	0.039	0.065
Mass and Area Correlation		0.910	0.887	0.934
Mass and Flying Distance Correlation		-0.197	-0.222	-0.197
Area and Flying Distance Correlation		-0.313	-0.304	-0.218
Sample Size		493	1070	994

Fire Ember Production from Wildland and Structural Fuels

Table 16. Firebrand Parameters for Wall-Roof Mockups: OSB Cladding Only, Combustible Roof

Physical Quantity	Statistical Quantity	Idle (5.36-m/s)	Medium Wind (11.17-m/s)	High Wind (17.88-m/s)
Flying Distance (m)	Mean	3.212	3.853	4.194
	Standard Deviation	3.306	3.398	4.643
	Skewness	1.611	1.599	1.413
	Median	2.530	2.910	2.028
Projected Area (cm ²)	Mean	2.201	2.066	3.923
	Standard Deviation	4.217	5.994	7.429
	Skewness	8.018	14.758	8.476
	Median	1.130	0.897	2.223
Mass (g)	Mean	0.159	0.263	0.393
	Standard Deviation	0.590	2.871	1.325
	Skewness	9.276	23.710	10.340
	Median	0.026	0.022	0.128
Mass and Area Correlation		0.969	0.411	0.948
Mass and Flying Distance Correlation		-0.206	-0.082	-0.142
Area and Flying Distance Correlation		-0.297	-0.206	-0.208
Sample Size		516	860	1000

Fire Ember Production from Wildland and Structural Fuels

Table 17. Firebrand Parameters for Wall-Roof Mockups: OSB Cladding Only, Noncombustible Roof

Physical Quantity	Statistical Quantity	Idle (5.36-m/s)	Medium Wind (11.17-m/s)	High Wind (17.88-m/s)
Flying Distance (m)	Mean	4.569	3.393	4.082
	Standard Deviation	4.056	3.531	4.052
	Skewness	0.960	1.519	1.513
	Median	2.910	2.028	2.028
Projected Area (cm ²)	Mean	2.017	2.894	3.502
	Standard Deviation	4.144	5.291	4.946
	Skewness	9.144	5.469	7.253
	Median	0.866	1.248	2.360
Mass (g)	Mean	0.149	0.235	0.306
	Standard Deviation	0.572	0.708	0.750
	Skewness	10.292	8.616	9.852
	Median	0.016	0.036	0.127
Mass and Area Correlation		0.968	0.955	0.947
Mass and Flying Distance Correlation		-0.244	-0.239	-0.155
Area and Flying Distance Correlation		-0.353	-0.319	-0.223
Sample Size		381	776	1131

Fire Ember Production from Wildland and Structural Fuels

Table 18. Firebrand Parameters for Wall-Roof Mockups: OSB Cladding Assembly, Combustible Roof

Physical Quantity	Statistical Quantity	Idle (5.36-m/s)	Medium Wind (11.17-m/s)	High Wind (17.88-m/s)
Flying Distance (m)	Mean	2.451	2.930	3.345
	Standard Deviation	2.870	3.672	4.106
	Skewness	1.910	1.849	1.660
	Median	1.158	1.470	1.158
Projected Area (cm ²)	Mean	2.467	2.388	3.754
	Standard Deviation	3.881	3.167	5.906
	Skewness	6.995	5.259	7.753
	Median	1.461	1.479	2.297
Mass (g)	Mean	0.191	0.182	0.350
	Standard Deviation	0.707	0.438	0.835
	Skewness	12.961	7.316	9.415
	Median	0.043	0.060	0.139
Mass and Area Correlation		0.900	0.961	0.969
Mass and Flying Distance Correlation		-0.140	-0.203	-0.174
Area and Flying Distance Correlation		-0.305	-0.276	-0.224
Sample Size		559	1004	1002

Fire Ember Production from Wildland and Structural Fuels

Table 19. Firebrand Parameters for Wall-Roof Mockups: OSB Cladding Assembly, Noncombustible Roof

Physical Quantity	Statistical Quantity	Idle (5.36-m/s)	Medium Wind (11.17-m/s)	High Wind (17.88-m/s)
Flying Distance (m)	Mean	2.445	4.304	4.927
	Standard Deviation	2.664	3.587	4.364
	Skewness	1.908	1.228	1.400
	Median	2.028	3.398	2.910
Projected Area (cm ²)	Mean	2.345	2.248	3.635
	Standard Deviation	4.471	3.523	7.478
	Skewness	7.804	5.031	8.861
	Median	0.882	0.984	1.838
Mass (g)	Mean	0.191	0.165	0.536
	Standard Deviation	0.586	0.484	6.586
	Skewness	8.554	8.594	33.213
	Median	0.022	0.024	0.103
Mass and Area Correlation		0.968	0.943	0.161
Mass and Flying Distance Correlation		-0.229	-0.273	-0.028
Area and Flying Distance Correlation		-0.292	-0.374	-0.226
Sample Size		540	584	1213

Fire Ember Production from Wildland and Structural Fuels

Table 20. Firebrand Parameters for Wall-Roof Mockups: Fiber Cement Cladding Assembly, Combustible Roof

Physical Quantity	Statistical Quantity	Idle (5.36-m/s)	Medium Wind (11.17-m/s)	High Wind (17.88-m/s)
Flying Distance (m)	Mean	3.617	2.626	5.412
	Standard Deviation	3.212	3.262	4.644
	Skewness	1.137	1.859	0.974
	Median	2.530	1.158	3.398
Projected Area (cm ²)	Mean	1.308	1.683	2.435
	Standard Deviation	2.253	2.798	2.642
	Skewness	9.062	9.000	3.425
	Median	0.694	0.995	1.571
Mass (g)	Mean	0.071	0.709	0.166
	Standard Deviation	0.310	17.701	0.309
	Skewness	15.115	29.461	5.701
	Median	0.013	0.027	0.068
Mass and Area Correlation		0.928	0.029	0.918
Mass and Flying Distance Correlation		-0.192	-0.026	-0.190
Area and Flying Distance Correlation		-0.361	-0.201	-0.285
Sample Size		452	870	1015

Fire Ember Production from Wildland and Structural Fuels

Table 21. Firebrand Parameters for Wall-Roof Mockups: Fiber Cement Cladding Assembly, Noncombustible Roof

Physical Quantity	Statistical Quantity	Idle (5.36-m/s)	Medium Wind (11.17-m/s)	High Wind (17.88-m/s)
Flying Distance (m)	Mean	2.550	3.455	4.254
	Standard Deviation	2.306	3.548	4.583
	Skewness	1.104	1.438	1.360
	Median	1.684	2.028	2.028
Projected Area (cm ²)	Mean	1.860	1.631	3.696
	Standard Deviation	2.963	2.686	4.993
	Skewness	4.795	7.161	4.593
	Median	0.860	0.815	2.187
Mass (g)	Mean	0.125	0.124	0.332
	Standard Deviation	0.379	0.556	0.798
	Skewness	6.272	18.310	7.710
	Median	0.018	0.019	0.119
Mass and Area Correlation		0.954	0.875	0.931
Mass and Flying Distance Correlation		-0.269	-0.155	-0.197
Area and Flying Distance Correlation		-0.390	-0.292	-0.291
Sample Size		364	867	866

E.2 Statistical Results for Collected Firebrands from Vegetative Fuels

Table 22. Measured Firebrand Parameters for Little Bluestem Grass

Physical Quantity	Statistical Quantity	Constant Wind	Variable Wind (Avg. & Gust Peak)	
		Idle (5.36-m/s)	Medium (11.17 & 14.30-m/s)	High (17.88 and 23.00-m/s)
Flying Distance (m)	Mean	1.146	1.712	3.429
	Standard Deviation	0.922	2.311	3.517
	Skewness	2.557	3.416	1.321
	Median	0.743	0.938	2.022
Projected Area (cm ²)	Mean	0.773	0.578	0.929
	Standard Deviation	0.576	0.403	0.664
	Skewness	4.150	3.631	2.856
	Median	0.657	0.509	0.735
Mass (g)	Mean	0.015	0.004	0.025
	Standard Deviation	0.021	0.007	0.037
	Skewness	2.407	6.761	4.767
	Median	0.007	0.003	0.013
Correlation	Mass and Area	0.547	0.764	0.659
	Mass and Flying Distance	-0.280	-0.047	-0.065
	Area and Flying Distance	-0.338	-0.167	-0.128
Sample Size		202	138	692

Fire Ember Production from Wildland and Structural Fuels

Table 23. Firebrand Parameters for Chamise

Physical Quantity	Statistical Quantity	Constant Wind	Variable Wind (Avg. & Gust Peak)	
		Idle (5.36-m/s)	Medium (11.17 & 14.30- m/s)	High (17.88 and 23.00-m/s)
Flying Distance (m)	Mean	1.403	1.205	3.318
	Standard Deviation	1.641	0.942	3.420
	Skewness	3.380	1.895	1.482
	Median	0.743	0.938	1.687
Projected Area (cm ²)	Mean	1.731	2.349	2.601
	Standard Deviation	1.923	2.460	2.568
	Skewness	4.567	4.466	3.705
	Median	1.306	1.712	1.843
Mass (g)	Mean	0.174	0.214	0.236
	Standard Deviation	0.592	0.568	0.539
	Skewness	11.070	6.401	5.182
	Median	0.048	0.061	0.067
Correlation	Mass and Area	0.849	0.906	0.875
	Mass and Flying Distance	-0.153	-0.231	-0.217
	Area and Flying Distance	-0.310	-0.346	-0.197
Sample Size		269	257	686

Fire Ember Production from Wildland and Structural Fuels

Table 24. Firebrand Parameters for Saw palmetto

Physical Quantity	Statistical Quantity	Constant Wind	Variable Wind (Avg. & Gust Peak)	
		Idle (5.36-m/s)	Medium (11.17 & 14.30- m/s)	High (17.88 and 23.00-m/s)
Flying Distance (m)	Mean	3.354	2.981	3.227
	Standard Deviation	3.212	3.305	3.412
	Skewness	1.499	1.666	1.611
	Median	2.101	1.587	1.687
Projected Area (cm ²)	Mean	1.255	1.789	2.346
	Standard Deviation	1.497	2.209	1.731
	Skewness	4.932	11.006	3.865
	Median	0.888	1.310	1.825
Mass (g)	Mean	0.018	0.020	0.081
	Standard Deviation	0.071	0.048	0.101
	Skewness	8.886	10.378	6.511
	Median	0.004	0.008	0.036
Correlation	Mass and Area	0.781	0.679	0.590
	Mass and Flying Distance	-0.106	-0.197	-0.129
	Area and Flying Distance	-0.186	-0.141	-0.148
Sample Size		938	1289	1230

Fire Ember Production from Wildland and Structural Fuels

Table 25. Firebrand Parameters for Loblolly pine

Physical Quantity	Statistical Quantity	Constant Wind	Variable Wind (Avg. & Gust Peak)	
		Idle (5.36-m/s)	Medium (11.17 & 14.30- m/s)	High (17.88 and 23.00-m/s)
Flying Distance (m)	Mean	1.493	2.998	4.093
	Standard Deviation	1.139	2.760	3.747
	Skewness	2.016	2.119	1.509
	Median	1.587	2.022	2.540
Projected Area (cm ²)	Mean	1.787	0.611	0.960
	Standard Deviation	3.569	0.879	1.096
	Skewness	6.687	3.808	3.520
	Median	0.915	0.329	0.613
Mass (g)	Mean	0.185	0.030	0.055
	Standard Deviation	0.845	0.073	0.134
	Skewness	11.646	6.941	5.707
	Median	0.038	0.008	0.019
Correlation	Mass and Area	0.915	0.891	0.905
	Mass and Flying Distance	-0.140	-0.236	-0.143
	Area and Flying Distance	-0.220	-0.306	-0.138
Sample Size		381	575	167

Fire Ember Production from Wildland and Structural Fuels

Table 26. Firebrand Parameters for Leyland cypress

Physical Quantity	Statistical Quantity	Constant Wind	Variable Wind (Avg. & Gust Peak)	
		Idle (5.36-m/s)	Medium (11.17 & 14.30- m/s)	High (17.88 and 23.00-m/s)
Flying Distance (m)	Mean	1.238	2.040	3.928
	Standard Deviation	0.739	1.989	2.657
	Skewness	1.327	2.529	1.099
	Median	0.938	1.587	2.474
Projected Area (cm ²)	Mean	1.881	1.745	2.371
	Standard Deviation	3.518	1.255	2.733
	Skewness	14.635	3.693	8.412
	Median	1.352	1.414	1.631
Mass (g)	Mean	0.191	0.108	0.283
	Standard Deviation	1.729	0.197	0.828
	Skewness	21.928	7.727	16.443
	Median	0.052	0.054	0.099
Correlation	Mass and Area	0.915	0.886	0.911
	Mass and Flying Distance	-0.068	-0.258	-0.300
	Area and Flying Distance	-0.147	-0.331	-0.333
Sample Size		529	883	1013